

Supporting Information
©Wiley-VCH 2016
69451 Weinheim, Germany

Abstract: Antimicrobial drug resistance demands novel approaches for improving the efficacy of antibiotics, especially against Gram-negative bacteria. Here we report that conjugating a diglycine (GG) to a prodrug of antibiotics drastically accelerates intrabacterial hydrolysis of ester bond for regenerating the antibiotics against *E. coli*. Specifically, the attachment of GG to chloramphenicol succinate (CLsu) generates a novel conjugate (CLsuGG), which exhibits about an order of magnitude higher inhibitory efficacy than CLsu against *E. coli*. Further studies reveal that CLsuGG undergoes rapid hydrolysis catalyzed by intrabacterial esterases (e.g., BioH and Yjfp) for generating chloramphenicol (CL) in *E. coli*. More importantly, the conjugate exhibits lower cytotoxicity to bone marrow stromal cells that CL does. The structural analogs of CLsuGG indicate that the conjugation of GG is an effective strategy for accelerating hydrolysis catalyzed by esterases and enhancing antibacterial efficacy of antibiotics. This work, for the first time, illustrates that dipeptide conjugation modulates intrabacterial hydrolysis for increasing antibiotic efficacy and reducing adverse drug effects.

DOI: 10.1002/anie.2016XXXXX

Table of Contents

S1. Experimental materials and instruments	3
S2. Synthesis and characterizations	3
S3. Hydrolysis assay	5
S4. TEM sample preparation	5
S5. Light scattering sample preparation	6
S6. Bacteria culture and inhibitory activity assay	6
S7. Cell culture and cell viability assay	6
S8. FLP-FRT recombination in <i>E. coli</i>	6
S9. Supplemental figures	7
Scheme S1. Synthesis of CLsuGG (3) by SPPS.	
Scheme S2. Synthesis of CLsuG (4) and CLsuGGG (5) by SPPS.	
Scheme S3. The synthetic route of compounds 6 and 7.	
Scheme S4. The synthetic route of compounds 8, 9, and 10.	
Scheme S5. The synthetic route of compound 11.	
Table S1. The minimum inhibitory concentration (MIC) summary of 1, 2, 3, 4, and 5.	
Figure S1. The hydrolysis curve of 2, 3, 4 and 5 by CES and the lysate of <i>E. coli</i> or HepG2.	
Figure S2. The LCMS spectrum of <i>E. coli</i> lysate with the addition of CLsuGG (3).	
Figure S3. TEM images of CLsuGG (3) before and after the addition of CES.	
Figure S4. The antibacterial activity of 3 against YdgR transporter knockout mutants of <i>E. coli</i> .	

Figure S5. The antibacterial activity of **3** against FepA transporter knockout mutants of *E. coli*.

Figure S6. The DNA gel electrophoresis image of double mutant *E. coli* with the deletion of BioH and Yjfp.

Figure S7. The growth rate of single esterase deletion mutants and a double esterase (BioH and Yjfp) deletion mutant of *E. coli*.

Figure S8. The antibacterial activity of **10** against BioH or Yjfp overexpressed mutants of *E. coli*.

Figure S9. Cell viability of HS-5, HepG2 and HEK293 cells incubated with **1**, **2** and **3** for 24 h.

Figure S10. The molecular structure of diglycine conjugated C-terminal of ciprofloxacin and its corresponding MIC value.

Figure S11. Cell viability of HS-5, HepG2, and HEK293 cells incubated with **6**, **7**, **8**, **9**, and **10** for 24 h.

Figure S12. The LC and Mass spectrum of CLsuGG (**3**).

Figure S13. The LC and Mass spectrum of CLsuG (**4**).

Figure S14. The LC and Mass spectrum of CLsuGGG (**5**).

Figure S15. The LC and Mass spectrum of **6**.

Figure S16. The LC and Mass spectrum of **7**.

Figure S17. The LC and Mass spectrum of **8**.

Figure S18. The LC and Mass spectrum of **9**.

Figure S19. The LC and Mass spectrum of **10**.

Figure S20. The LC and Mass spectrum of **11**.

Figure S21. ^1H NMR of CLsuGG (**3**) in DMSO- d_6 .

Figure S22. ^{13}C NMR of CLsuGG (**3**) in DMSO- d_6 .

Figure S23. ^1H NMR of CLsuG (**4**) in DMSO- d_6 .

Figure S24. ^{13}C NMR of CLsuG (**4**) in DMSO- d_6 .

Figure S25. ^1H NMR of CLsuGGG (**5**) in DMSO- d_6 .

Figure S26. ^{13}C NMR of CLsuGGG (**5**) in DMSO- d_6 .

Figure S27. ^1H NMR of **6** in DMSO- d_6 .

Figure S28. ^{13}C NMR of **6** in DMSO- d_6 .

Figure S29. ^1H NMR of **7** in DMSO- d_6 .

Figure S30. ^{13}C NMR of **7** in DMSO- d_6 .

Figure S31. ^1H NMR of **8** in DMSO- d_6 .

Figure S32. ^{13}C NMR of **8** in DMSO- d_6 .

Figure S33. ^1H NMR of **9** in DMSO- d_6 .

Figure S34. ^{13}C NMR of **9** in DMSO- d_6 .

Figure S35. ^1H NMR of **10** in DMSO- d_6 .

Figure S36. ^{13}C NMR of **10** in DMSO- d_6 .

Figure S37. ^1H NMR of **11** in DMSO- d_6 .

Figure S38. ^{13}C NMR of **11** in DMSO- d_6 .

S1. Experimental materials and instruments

All the solvents and chemical reagents were used directly as received from the commercial sources without further purification unless otherwise stated. Carboxylesterase (CES) from porcine liver was purchased from Sigma-Aldrich (lyophilized powder, ≥ 15 units/mg solid; Unit definition: One unit will hydrolyze 1.0 μ mol of ethyl butyrate to butyric acid and ethanol per min at pH 8.0 at 25 °C). CLsuGG (**3**), CLsuG (**4**), CLsuGGG (**5**), **6**, **7**, **8**, **9**, and **10** were purified with Agilent 1100 Series Liquid Chromatography system, equipped with an XTerra C18 RP column and Variable Wavelength detector. The LC-MS spectra were obtained with a Waters Acquity Ultra Performance LC with Waters MICROMASS detector. ^1H NMR spectra were obtained on Varian Unity Inova 400, and TEM images on a Morgagni 268 transmission electron microscope.

S2. Synthesis and characterizations

We synthesized CLsu (**2**) by acidifying the commercially available chloramphenicol succinate sodium. Chloramphenicol succinate sodium (150 mg) was dissolved in distilled water (3 mL), and HCl (1 M) was added dropwise until the pH of the mixture was adjusted to 2.0. The precipitate was washed several times with distilled water and dried for further use.

We used solid phase peptide synthesis (SPPS)^[1] for the synthesis of CLsuGG (**3**), CLsuG (**4**), and CLsuGGG (**5**). As shown in Scheme S1 and S2, we used 2-chlorotrityl chloride resin and N-Fmoc-glycine for the synthesis. Then we used CLsu (**2**) to cap the N-terminal of the peptides. After cleaving the compounds from resin, we purified all compounds (yields of **3**, **4** and **5**: up to 90%) by reverse phase HPLC using HPLC grade acetonitrile and water with supplement of 0.1% trifluoroacetic acid as the eluents.

CLsuGG (**3**): ^1H NMR (400 MHz, DMSO- d_6 , 25 °C, ppm): δ 8.51 (d, J = 8.0 Hz, 1H), 8.17 (m, 4H), 7.64 (d, J = 12.0 Hz, 2H), 6.44 (s, 1H), 5.02 (s, 1H), 4.21 (m, 2H), 4.10 (m, 1H), 3.74 (dd, J = 4.0, 8.0 Hz, 4H), 2.48 (m, 4H); ^{13}C NMR (100 MHz, DMSO- d_6 , 25 °C, ppm): δ 172.63, 171.53, 169.73, 164.04, 150.67, 147.02, 127.89, 123.32, 69.88, 66.70, 63.44, 53.93, 42.24, 40.97, 30.09, 29.33; ESI-MS m/z calcd. for $\text{C}_{19}\text{H}_{22}\text{Cl}_2\text{N}_4\text{O}_{10}$ [M]⁺: m/z = 537.30, found [M-H]⁻: 535.24.

CLsuG (**4**): ^1H NMR (400 MHz, DMSO- d_6 , 25 °C, ppm): δ 8.51 (d, J = 8.0 Hz, 1H), 8.24 (t, J = 4.0 Hz, 1H), 8.17 (d, J = 12.0 Hz, 2H), 7.64 (d, J = 8.0 Hz, 2H), 6.44 (s, 1H), 5.03 (s, 1H), 4.21 (m, 2H), 4.10 (m, 1H), 3.75 (d, J = 4.0 Hz, 2H), 2.46 (m, 4H); ^{13}C NMR (100 MHz, DMSO- d_6 , 25 °C, ppm): δ 172.51, 171.72, 171.55, 164.04, 150.69, 147.02, 127.89, 123.31, 69.85, 66.70, 63.40, 53.91, 41.05, 29.94, 29.31; ESI-MS m/z calcd. for $\text{C}_{17}\text{H}_{19}\text{Cl}_2\text{N}_3\text{O}_9$ [M]⁺: m/z = 480.25, found [M-H]⁻: 478.10.

CLsuGGG (**5**): ^1H NMR (400 MHz, DMSO- d_6 , 25 °C, ppm): δ 8.51 (d, J = 8.0 Hz, 1H), 8.17 (m, 5H), 7.64 (d, J = 8.0 Hz, 2H), 6.44 (s, 1H), 5.03 (s, 1H), 4.22 (m, 2H), 4.10 (m, 1H), 3.75 (m, 7H), 2.47 (m, 4H); ^{13}C NMR (100 MHz, DMSO- d_6 , 25 °C, ppm): δ 172.62, 171.70, 171.48, 169.68, 169.55, 164.05, 150.67, 147.02, 127.88, 123.32, 69.89, 66.70, 63.45, 53.93, 42.57, 42.14, 40.97, 30.09, 29.33; ESI-MS m/z calcd. for $\text{C}_{21}\text{H}_{25}\text{Cl}_2\text{N}_5\text{O}_{11}$ [M]⁺: m/z = 594.36, found [M-H]⁻: 592.09.

Synthesis of compound 6. As shown in Scheme S3, CL (**1**) (323.1 mg, 1.0 mmol), *trans*-1,2-cyclohexanedicarboxylic anhydride (169.6 mg, 1.1 mmol), and 4-(dimethylamino)pyridine (24.4 mg, 0.2 mmol) were dissolved in THF (4 mL) and stirred at 50 °C overnight. After that, the solution was cooled to the room temperature, and THF was removed. The crude product was used for SPPS without further purification. The cell culture grade of compound **6** (yield: 79%) was purified by reverse phase HPLC using HPLC grade acetonitrile and water with supplement of 0.1% trifluoroacetic acid as the eluents. ^1H NMR (400 MHz, DMSO- d_6 , 25 °C, ppm): δ

8.53 (dd, $J = 12.0, 8.0$ Hz, 1H), 8.16 (d, $J = 8.0$ Hz, 2H), 7.62 (d, $J = 8.0$ Hz, 2H), 6.43 (m, 1H), 5.01 (s, 1H), 4.24 (m, 2H), 4.16 (d, $J = 8.0$ Hz, 1H), 4.00 (t, $J = 8.0$ Hz, 1H), 2.45 (m, 2H), 1.93 (d, $J = 28.0$ Hz, 2H), 1.67 (s, 2H), 1.23 (s, 4H); ^{13}C NMR (100 MHz, DMSO- d_6 , 25 °C, ppm): δ 176.24, 174.55, 163.95, 150.57, 147.03, 127.87, 123.32, 69.89, 66.72, 63.31, 54.08, 53.78, 44.65, 44.51, 28.78, 25.22; ESI-MS m/z calcd. for $\text{C}_{19}\text{H}_{22}\text{Cl}_2\text{N}_2\text{O}_8$ [M] $^+$: $m/z = 477.29$, found [M-H] $^-$ 475.13.

Synthesis of compound 7. As shown in Scheme S3, we used 2-chlorotrityl chloride resin and N-Fmoc-glycine for the synthesis. Then we used compound **6** to cap the N-terminal of the peptides. After cleaving the compounds from resin, we purified compound **7** (yield: 71%) by reverse phase HPLC using HPLC grade acetonitrile and water with supplement of 0.1% trifluoroacetic acid as the eluents. ^1H NMR (400 MHz, DMSO- d_6 , 25 °C, ppm): δ 8.51(dd, $J = 8.0, 24.0$ Hz, 1H), 8.15 (m, 3H), 7.94 (m, 1H), 7.63 (m, 2H), 6.44 (d, $J = 12.0$ Hz, 1H), 5.00 (d, $J = 16.0$ Hz, 1H), 4.08 (m, 3H), 3.71 (m, 4H), 2.45 (m, 2H), 1.92 (s, 2H), 1.68 (s, 2H), 1.22 (m, 4H); ^{13}C NMR (100 MHz, DMSO- d_6 , 25 °C, ppm): δ 174.97, 174.79, 171.53, 169.69, 164.02, 150.74, 147.01, 127.87, 123.32, 69.76, 66.72, 63.29, 53.71, 45.44, 44.79, 42.10, 40.98, 29.75, 29.07, 25.36; ESI-MS m/z calcd. for $\text{C}_{23}\text{H}_{28}\text{Cl}_2\text{N}_4\text{O}_{10}$ [M] $^+$: $m/z = 591.40$, found [M-H] $^-$ 589.23.

Synthesis of compound 8. As shown in Scheme S4, glycolic acid (106.5 mg, 1.4 mmol) and HBTU (530.9 mg, 1.4 mmol) dissolved in DMF (4 mL) and stirred for 30 min, followed by adding ciprofloxacin (331.3 mg, 1.0 mmol) and N,N-diisopropylethylamine (500 μL , 3.0 mmol) in the solution and stirring continuously overnight. Compound **8** (yield: 90%) was purified by silica gel chromatography (1% MeOH in CH_2Cl_2). ^1H NMR (400 MHz, DMSO- d_6 , 25 °C, ppm): δ 8.66 (s, 1H), 7.93 (d, $J = 12.0$ Hz, 1H), 7.58 (d, $J = 8.0$ Hz, 1H), 4.16 (s, 2H), 3.82 (m, 1H), 3.65 (m, 4H), 3.34 (s, 4H), 1.32 (m, 2H), 1.19 (m, 2H); ^{13}C NMR (100 MHz, DMSO- d_6 , 25 °C, ppm): δ 176.79, 170.64, 166.31, 154.60, 152.13, 148.50, 145.27, 139.55, 119.31, 111.56, 111.33, 107.19, 60.62, 49.83, 43.74, 36.31, 8.02; ESI-MS m/z calcd. for $\text{C}_{19}\text{H}_{20}\text{FN}_3\text{O}_5$ [M] $^+$: $m/z = 389.38$, found [M-H] $^-$ 388.08.

Synthesis of compound 9. As shown in Scheme S4, compound **8** (110.0 mg, 0.3 mmol), succinic anhydride (39.6 mg, 0.4 mmol), and N,N-diisopropylethylamine (234 μL , 1.5 mmol) were dissolved in DMF (1 mL) and stirred at 40 °C overnight. Compound **9** (yield: 83%) was purified by reverse phase HPLC using HPLC grade acetonitrile and water with supplement of 0.1% trifluoroacetic acid as the eluents. ^1H NMR (400 MHz, DMSO- d_6 , 25 °C, ppm): δ 8.67 (s, 1H), 7.93 (d, $J = 12.0$ Hz, 1H), 7.59 (d, $J = 8.0$ Hz, 1H), 4.87 (s, 2H), 3.83 (s, 1H), 3.65 (d, $J = 16.0$ Hz, 4H), 3.35 (d, $J = 16.0$ Hz, 4H), 2.62 (dd, $J = 8.0, 4.0$ Hz, 2H), 2.51 (m, 2H), 1.32(m, 2H), 1.19 (m, 2H); ^{13}C NMR (100 MHz, DMSO- d_6 , 25 °C, ppm): δ 176.81, 173.64, 172.15, 166.32, 165.33, 154.61, 152.13, 148.53, 145.32, 145.21, 139.56, 119.29, 111.58, 111.35, 107.20, 61.89, 49.84, 43.97, 36.32, 29.07, 8.03; ESI-MS m/z calcd. for $\text{C}_{23}\text{H}_{24}\text{FN}_3\text{O}_8$ [M] $^+$: $m/z = 489.46$, found [M-H] $^-$ 488.33.

Synthesis of compound 10. As shown in Scheme S4, compound **9** (120.0 mg, 0.25 mmol), diglycine (64.8 mg, 0.49 mmol), N-hydroxysuccinimide (28.3 mg, 0.25 mmol), N,N-diisopropylethylamine (200 μL , 1.23 mmol), and polymer supported-DCC (700.0 mg, 1.0-2.0 mmol/g loading) were poured in CHCl_3 (2 mL) and the reaction suspension was stirred at 40 °C for 4 h. The resulting mixture was filtered, and the resin was washed several times with CH_2Cl_2 . The filtrate was evaporated under reduced pressure and was purified by reverse phase HPLC (yield: 29%) using HPLC grade acetonitrile and water with supplement of 0.1% trifluoroacetic acid as the eluents. ^1H NMR (400 MHz, DMSO- d_6 , 25 °C, ppm): δ 8.67 (s, 1H), 8.24 (dd, $J = 8.0, 4.0$ Hz, 1H), 8.10 (dd, $J = 4.0, 8.0$ Hz, 1H), 7.95 (d, $J = 12.0$ Hz, 1H), 7.59 (d, $J = 8.0$ Hz, 2H), 4.86 (s, 2H), 3.83 (m, 1H), 3.74 (m, 4H), 3.65 (m, 5H), 3.41 (m, 2H), 2.63 (dd, $J = 8.0, 4.0$ Hz, 2H), 2.47 (m, 2H), 1.32 (m, 2H), 1.19 (m, 2H); ^{13}C NMR (100 MHz, DMSO- d_6 , 25 °C, ppm): δ 176.80, 172.45, 171.53,

171.43, 169.72, 166.31, 165.39, 154.61, 152.13, 148.52, 145.31, 139.55, 119.35, 111.57, 111.34, 107.20, 61.82, 49.82, 43.96, 36.31, 30.20, 29.25; ESI-MS m/z calcd. for $C_{27}H_{30}FN_5O_{10}$ [M]⁺: m/z = 603.56, found [M-H]⁻ 602.29.

Synthesis of compound 11. To a solution of ciprofloxacin (663.0 mg, 2.0 mmol) in a 1:1 mixture of THF-H₂O (10 mL-10 mL), NaHCO₃ (672.0 mg, 8.0 mmol) and di-tert-butyl dicarbonate (523.0 mg, 2.4 mmol) were added consecutively at 0 °C with magnetic stirring. After 30 min, the reaction mixture was allowed to attain room temperature and stirring continued overnight. The turbid solution was extracted with ethyl acetate (2×100 mL). The aqueous layer was acidified to pH = 4-5 by careful addition of half saturated cold citric acid and then extracted with methylene chloride (3×100 mL). The combined organic phase was dried over anhydrous Na₂SO₄ and evaporated under reduced pressure to give the Boc-protected ciprofloxacin. The crude product was used for SPPS without further purification. Then we used the Boc-protected ciprofloxacin to cap the N-terminal of the diglycine. After cleaving the compounds from resin, we purified compound **11** by reverse phase HPLC using HPLC grade acetonitrile and water with supplement of 0.1% trifluoroacetic acid as the eluents. ¹H NMR (400 MHz, DMSO-*d*₆, 25 °C, ppm): δ 12.58 (s, 1H), 10.13 (dd, *J* = 4.0, 8.0 Hz, 1H), 8.95 (s, 1H), 8.64 (s, 1H), 8.33 (dd, *J* = 8.0, 4.0 Hz, 1H), 7.92 (d, *J* = 12.0 Hz, 1H), 7.53 (d, *J* = 8.0 Hz, 1H), 4.04 (d, *J* = 4.0 Hz, 2H), 3.79 (d, *J* = 8.0 Hz, 2H), 3.75 (m, 1H), 3.48 (m, 4H), 3.30 (m, 4H), 1.31 (m, 2H), 1.12 (m, 2H); ¹³C NMR (100 MHz, DMSO-*d*₆, 25 °C, ppm): δ 174.54, 171.55, 169.41, 164.38, 154.18, 151.72, 147.32, 143.55, 138.74, 122.01, 121.94, 112.01, 111.78, 110.51, 107.08, 47.03, 43.15, 42.39, 41.04, 35.50, 8.02; ESI-MS m/z calcd. for $C_{21}H_{24}FN_5O_5$ [M]⁺: m/z = 445.45, found [M-H]⁻ 444.38.

S3. Hydrolysis assay

Wild-type *E. coli* strains (K12) were harvested by centrifugation and the cell pellets were lysed using a sonic device. After centrifugation, the supernatant was collected and the proteinase inhibitor was added in the *E. coli* lysate. The concentration of *E. coli* lysate was normalized by the fluorescence intensity of 5-carboxyfluorescein diacetate (CFDA). Briefly, different concentrations of CES (4 U/mL, 2 U/mL, 1 U/mL, 0.5 U/mL, 0.25 U/mL, 0.125 U/mL, 0.0625 U/mL, 0.03125 U/mL, 0.015625 U/mL and 0 U/mL) and different amount of *E. coli* lysates were prepared in PBS buffer. Followed by, 25 μM of CFDA was added in and incubated at room temperature for 1 h. Then the fluorescence was tested to draw a fluorescence-concentration dependent curve for figuring out the concentration of *E. coli* lysates. Solutions of CLsuGG (**3**) (200 μM) were prepared in pH 7.4 PBS buffer. CES and *E. coli* lysate (0.1 U/mL) were added and incubated with above solutions at 37 °C for 24 h. At different time points, the solution was taken out, extracted with an equal volume of butanol, concentrated to dryness, and resuspended with butanol for HPLC analysis. HPLC was performed with Agilent 1100 Series Liquid Chromatograph equipped with an XTerra C18 reverse phase column and Variable Wavelength Detector. The hydrolyzed mixture resuspended in 1 mL of butanol was injected to HPLC mobile phase (0.1% trifluoroacetic acid, the starting ratio: 10% acetonitrile and 90% water). The system was run at a flow rate of 10 mL/min. Sample detection was achieved at 220 nm.

S4. TEM sample preparation

In this paper, we used negative staining technique to study the TEM images. We first glow discharged the 400 mesh copper grids coated with continuous thick carbon film (~ 35 nm) prior to use to increase the hydrophilicity. After loading samples (7 μL) on the grid,

we then rinsed grid by dd-water for twice or three times. Immediately after rinsing, we stained the grid containing sample with 2.0 % w/v uranyl acetate for three times. Afterwards, we allowed the grid to dry in air.

S5. Light scattering sample preparation

The static light scattering experiments were performed by using an ALV (Langen, Germany) goniometer and correlator system with a 22 mW HeNe ($\lambda = 633$ nm) laser and an avalanche photodiode detector. All samples were dissolved in PBS buffer. The addition of CES to the solution of **3** for 24 h, we obtained corresponding enzymatic hydrolyzed samples. The SLS tests were carried out at room temperature, and the angles of light scattering we chose were 30°, 60°, 90° and 120°, respectively. The resulting intensity ratios are proportional to the amount of aggregates in the samples.

S6. Bacteria culture and inhibitory activity assay

Single esterase (BioH, Yjfp, FrsA, YbfF, YfbB, YqiA, YeiG, or and YpfH) deletion mutants were purchased from Dharmacon Horizon Discovery (Cambridge, United Kingdom). The K12 wild-type *E. coli* strain (MG1655) was cultured in autoclaved LB medium (25 g/L LB broth/water) in a shaker-incubator overnight to stationary growth phase, and then sub-cultured in the same medium after dilution to OD₆₀₀ of 0.05. Compounds were added at different concentrations. The mixture of bacteria and compounds were placed (200 μ L/well) into 96-well clear flat bottom plates. In all plates, the OD₆₀₀ was measured before and after 16 h incubation at 37 °C.^[2]

S7. Cell culture and cell viability assay

All mammalian cell lines were purchased from the American Type Culture Collection (ATCC, Manassas, VA, USA). The HS-5 and HEK293T cells were propagated in Dulbecco's Modified Eagle's Medium (DMEM) supplemented with 10% fetal bovine serum (FBS) and 1% antibiotics in a fully humidified incubator containing 5% CO₂ at 37°C, HepG2 cells in Eagle's Minimum Essential Media (MEM) supplemented with 10% FBS and 1% antibiotics in a fully humidified incubator containing 5% CO₂ at 37°C.

Cells in exponential growth phase were seeded in a 96 well plate at a concentration of 1×10^4 cell/well, and were allowed to attach to the well for 24 h at 37°C, 5% CO₂. The culture medium was removed and 100 μ L culture medium containing corresponding compounds (immediately diluted from fresh prepared stock solution) at gradient concentrations (0 μ M as the control) was placed into each well. After culturing at 37°C, 5% CO₂ for 24h, 48h and 72h, each well was added with 10 μ L of 5 mg/mL MTT ((3-(4,5-dimethylthiazol-2-yl)-2,5-diphenyltetrazolium bromide), and the plated cells were incubated at dark for 4h. 100 μ L 10% SDS with 0.01M HCl was added to each well to stop the reduction and to dissolve the purple. After incubation of the cells at 37°C for overnight, the OD at 595 nm of the solution was measured in a microplate reader. Data represent the mean \pm standard deviation of three independent experiments.

S8. FLP-FRT recombination in *E. coli*

We used FLP-FRT recombination to generate double gene knockout mutants.

Day1: Transform recombinase plasmid

1. Make electrocompetent cells of the desired *E. coli* strain.
2. Transform with pCP20. This plasmid has a temperature-sensitive origin of replication, confers ampicillin resistance, and encodes the FLP recombinase.
3. Add 1 mL SOC and incubate in a tube shaking on its side at ≥ 120 rpm for 1 h at 30 °C to allow antibiotic resistance induction.
4. Plate 100 μL , 200 μL of the culture on an LB + Amp plate, respectively.
5. Grow overnight at 30 °C.

Day 2: Induce recombination

1. Pick a single colony from the LB + Amp plate.
2. Inoculate into 5 mL of LB medium in a test tube.
3. Grow overnight at 43 °C to induce FLP recombinase expression and select for loss of pCP20.

Day 3: Plate to get single candidate recombinants

1. Make a 10^6 dilution of the overnight culture.
2. Plate 50 μL of this dilution on LB plate.
3. Grow overnight at 30 °C to prevent partial loss of plasmid from colonies founded by cells that did not lose plasmid.

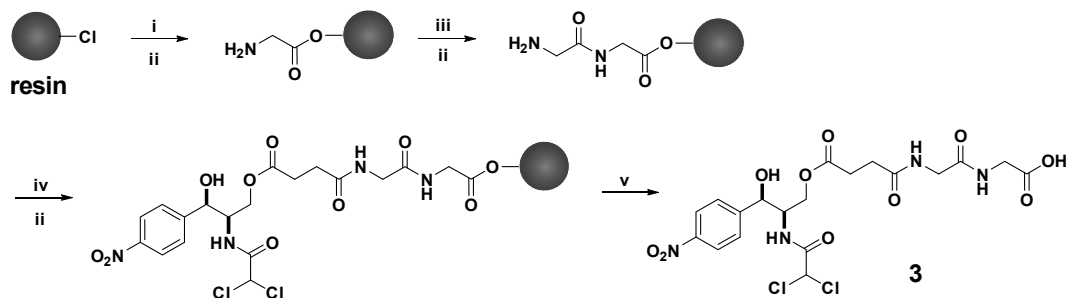
Day 4: Screen for genomic recombination and plasmid loss

1. Patch six individual colonies from this plate onto LB + Kan, LB + Amp and LB plates, respectively. Do the patching by picking a colony then streaking a small spot on each plate in this order.
2. Grow overnight at 37 °C for LB and LB + Kan and grow at 30 °C for LB + Amp plates.

Day 5: Grow up successful recombinants

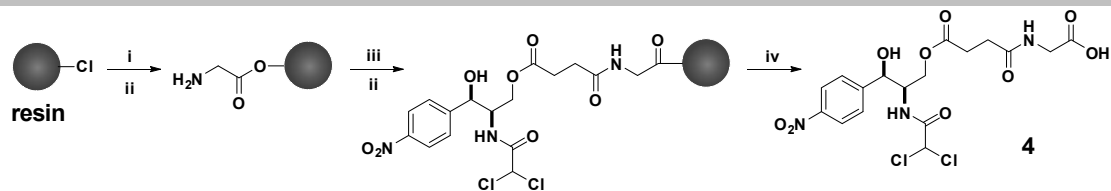
1. Inoculate 5 mL LB medium from patches on LB plates that score as sensitive to both antibiotics.
2. Grow overnight at 37 °C, shaking at 120 rpm.

S9. Supplemental figures

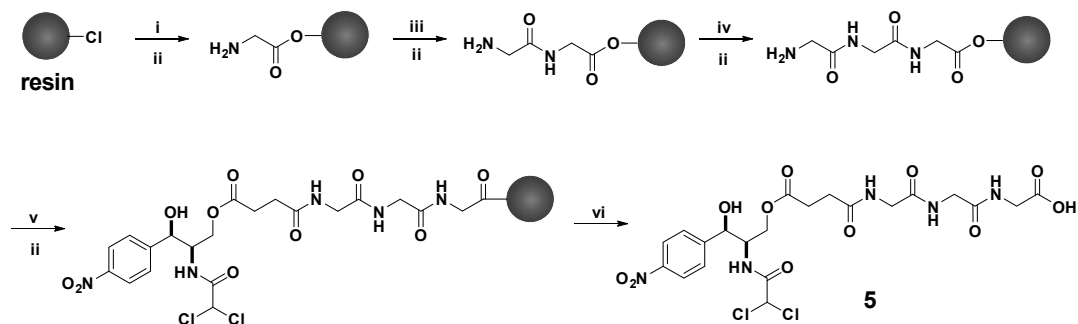


i) Fmoc-Gly-OH, DIEA; ii) 20% Piperidine; iii) Fmoc-Gly-OH, HBTU, DIEA; iv) CLRP, HBTU, DIEA; v) TFA.

Scheme S1. Synthesis of CLsuGG (**3**) by SPPS.

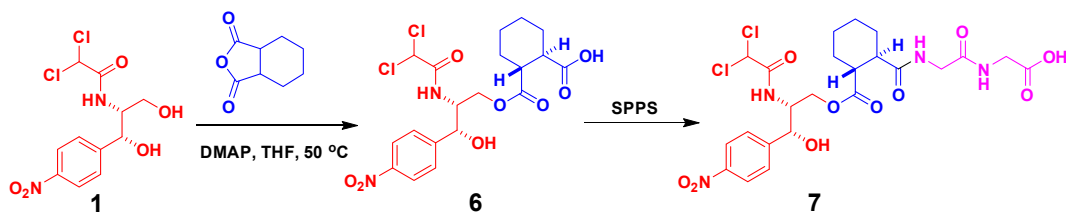


i) Fmoc-Gly-OH, DIEA; ii) 20% Piperidine; iii) CLRP, HBTU, DIEA; iv) TFA.

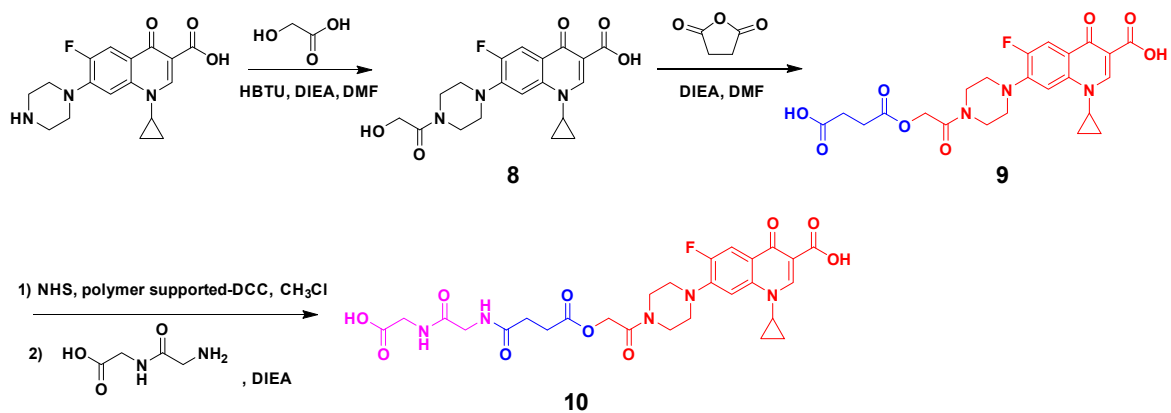


i) Fmoc-Gly-OH, DIEA; ii) 20% Piperidine; iii) Fmoc-Gly-OH, HBTU, DIEA; iv) Fmoc-Gly-OH, HBTU, DIEA; v) CLRP, HBTU, DIEA; vi) TFA.

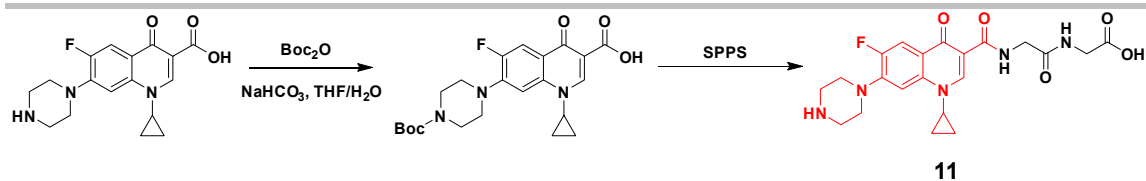
Scheme S2. Synthesis of CLsuG (**4**) and CLsuGGG (**5**) by SPPS.



Scheme S3. The synthetic route of compound **6** and **7**.



Scheme S4. The synthetic route of compound **8**, **9**, and **10**.



Scheme S5. The synthetic route of compound **11**.

Table S1. The minimum inhibitory concentration (MIC) summary of **1**, **2**, **3**, **4**, and **5**.

Entry	Compound	MIC (μM)	MIC ($\mu\text{g/mL}$)
1	CL (1)	20	6.5
2	CLsu (2)	>200	>84.6
3	CLsuGG (3)	20	10.7
4	CLsuG (4)	>200	>95.8
5	CLsuGGG (5)	20	11.9

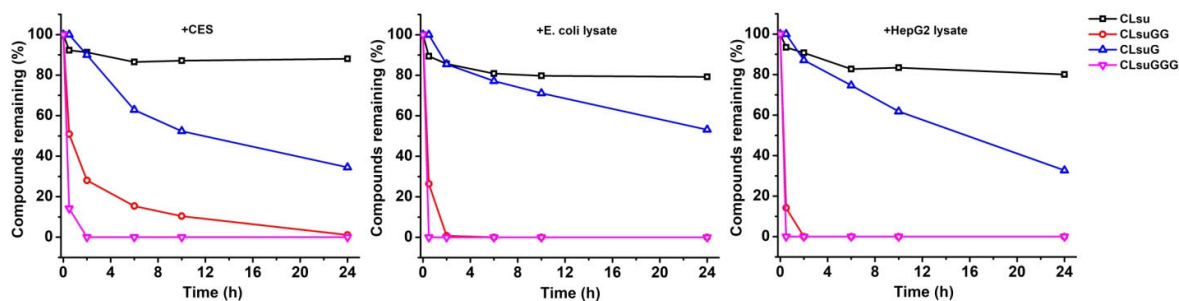


Figure S1. (A) The hydrolysis curve of **2**, **3**, **4** and **5** with the addition of (A) CES and the lysate of (B) *E. coli* (K-12) or (C) HepG2. [2]
 = [3] = [4] = [5] = 200 μM , [CES] = [*E. coli* lysate] = [HepG2 lysate] = 0.1 U/mL.

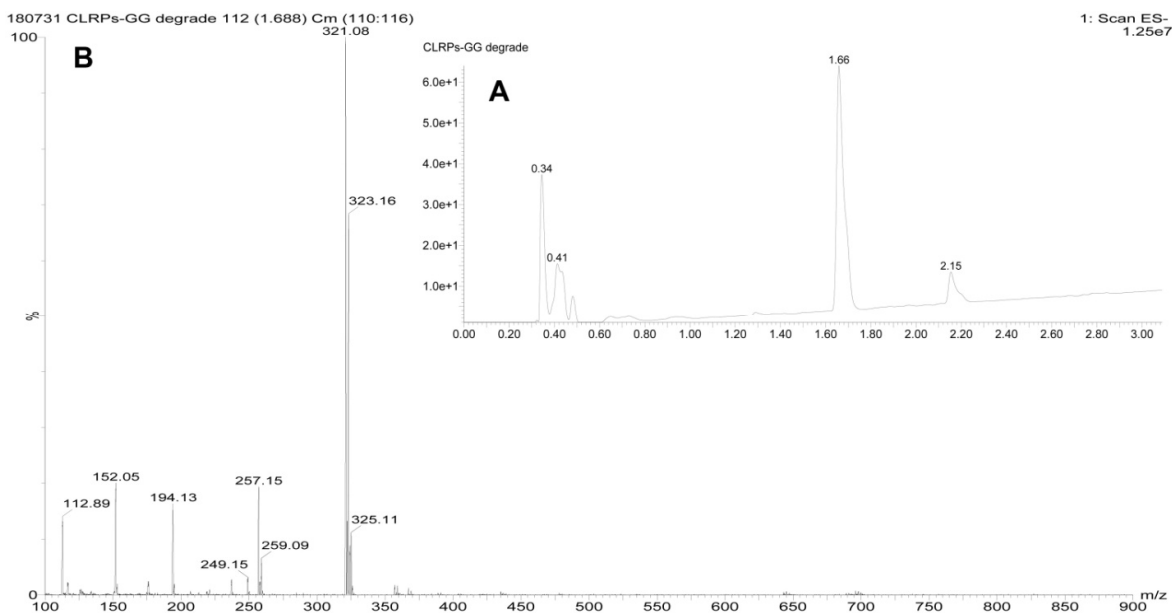


Figure S2. (A) The LC spectrum of *E. coli* lysate with the addition of CLSuGG (**3**) at the concentration of 500 μM show **3** completely degraded into chloroamphenicol (r.t. = 1.66 min). (B) The MS spectrum of *E. coli* lysate with the addition of CLSuGG shows the presence of chloroamphenicol (r.t. = 1.66 min), which is at m/z 321.08 [M-H]⁻. *E. coli* strains were harvested by centrifugation and the cell pellets were lysed using a sonic device. After centrifugation, **3** was added to the cell extracts, which were then stored at 37 °C for 24h. To terminate the reactions, the solution was extracted with an equal volume of butanol and then concentrated to dryness before resuspended with butanol.

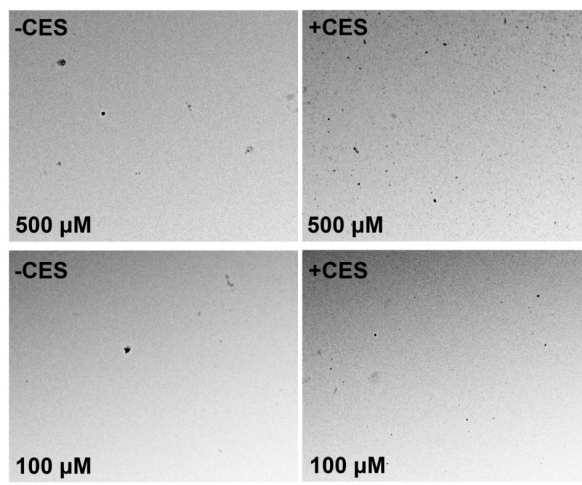


Figure S3. TEM images of CLSuGG (500 μM and 100 μM) show little nanoparticles before the addition of CES, whereas appear lots of nanoparticles after the addition of CES (1 U/mL), scale bar = 500 nm.

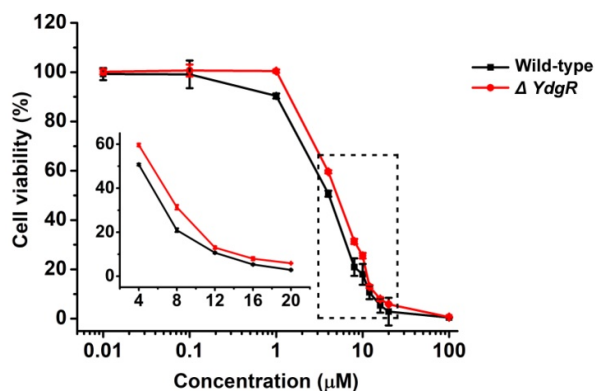


Figure S4. The antibacterial activity of **3** against YdgR transporter knockout mutants of *E. coli* (inset: corresponding magnified image of dash line square).

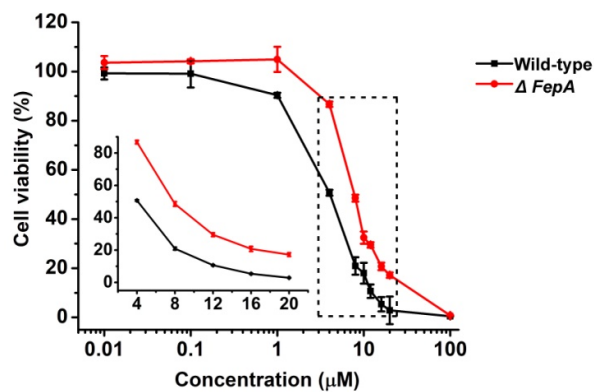


Figure S5. The antibacterial activity of **3** against FepA transporter knockout mutants of *E. coli* (inset: corresponding magnified image of dash line square).

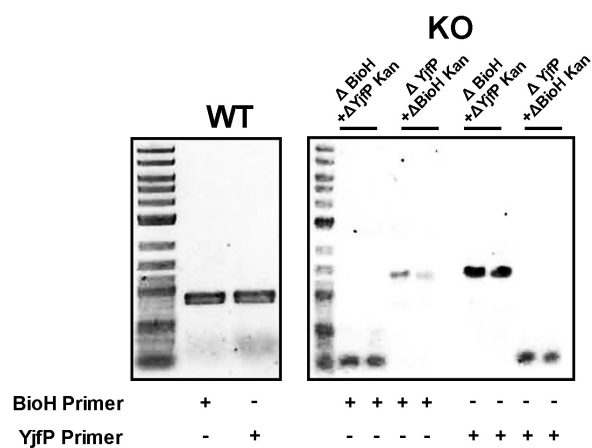


Figure S6. The 0.8 % TAE agarose DNA gel electrophoresis image shows confirmation of double mutant *E. coli* with the deletion of BioH and Yjfp. Two single colonies per mutant were picked randomly to do PCR.

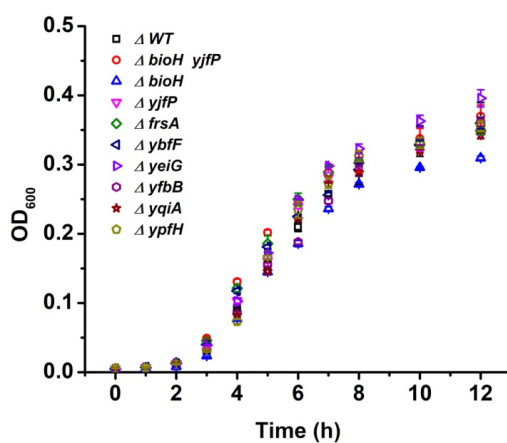


Figure S7. The growth rate of single esterase (BioH, Yjfp, FrsA, YbFF, YfbB, YqiA, YeiG, or YpfH) deletion mutants and a double esterase (BioH and Yjfp) deletion mutant of *E. coli* confirms the overall fitness of mutants.

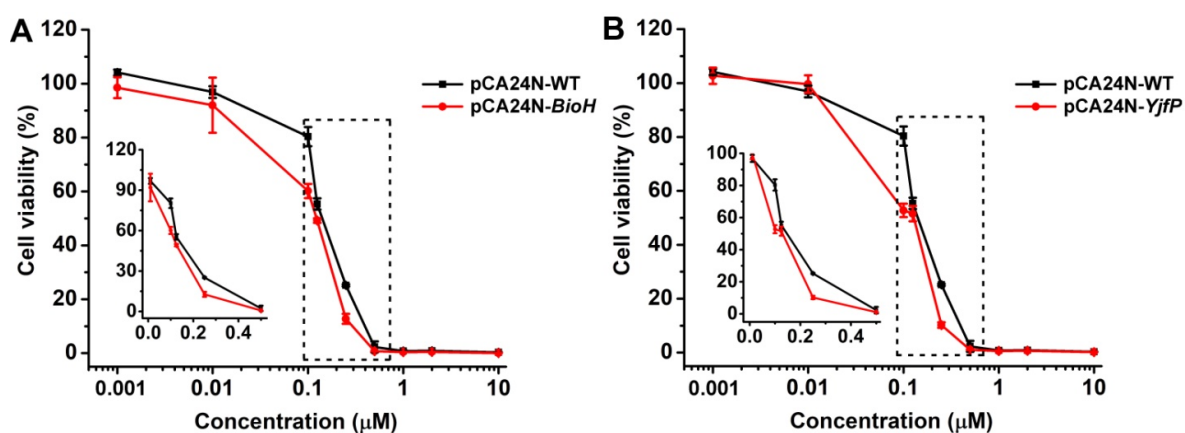


Figure S8. The antibacterial activity of **10** against (A) BioH and (B) Yjfp overexpressed mutants of *E. coli* (inset: corresponding magnified image of dash line square). pCA24N-WT: wild type plus plasmid pCA24N; pCA24N-BioH: wild type plus plasmid pCA24N-BioH; pCA24N-Yjfp: wild type plus plasmid pCA24N-Yjfp. Isopropyl thiogalactose (IPTG) is used for the induction of the expression of recombinant proteins in *E. coli* and pretreated the mutants for 1 h. [IPTG] = 1 mM.

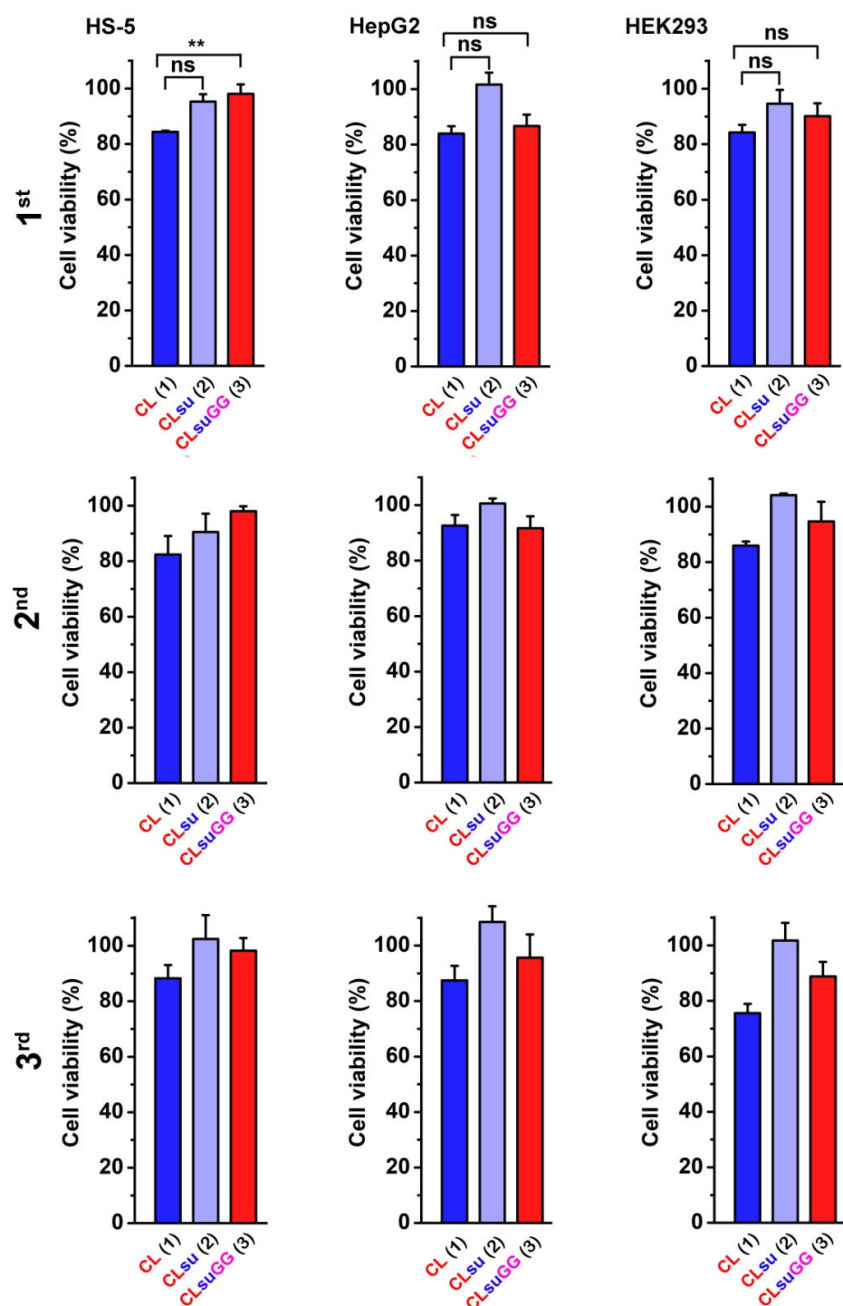


Figure S9. Three times-independent cell viability of HS-5, HepG2 and HEK293 cells incubated with 1, 2 and 3 for 24 h confirms the repeatability, [1] = [2] = [3] = 20 μ M (**= $p \leq 0.01$, ns= $p > 0.5$).

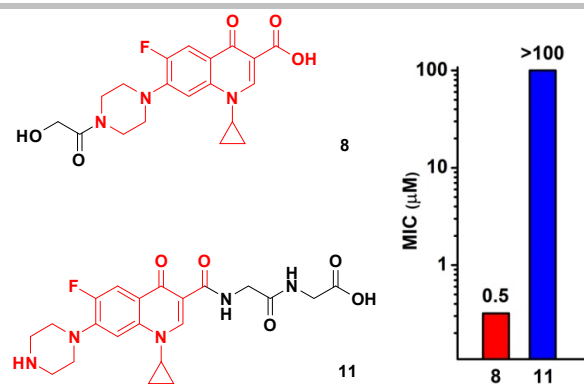


Figure S10. The molecular structures of N-terminal and C-terminal modified ciprofloxacin, and their corresponding MIC values against a wild type *E. coli* strain (K12).

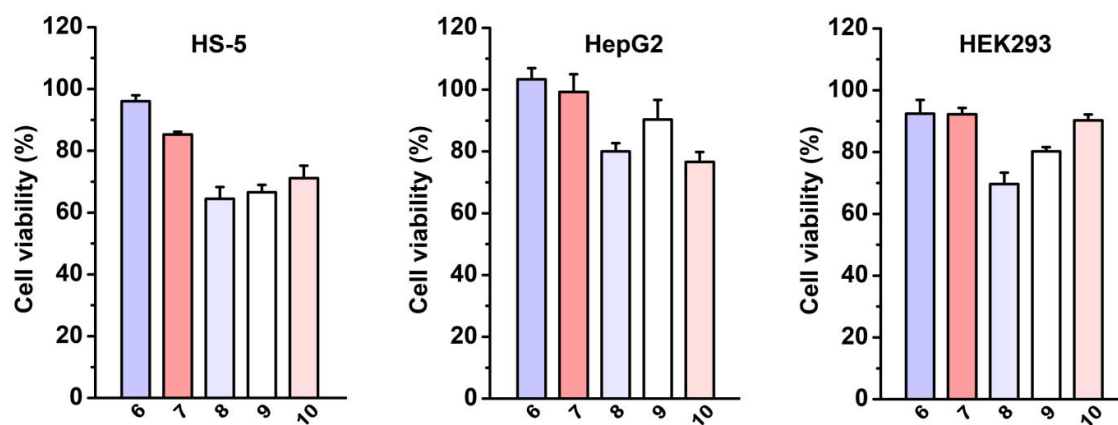


Figure S11. Cell viability of HS-5, HepG2 and HEK293 cells incubated with 6, 7, 8, 9 and 10 for 24 h, [6] = [7] = [8] = [9] = [10] = 20 μM .

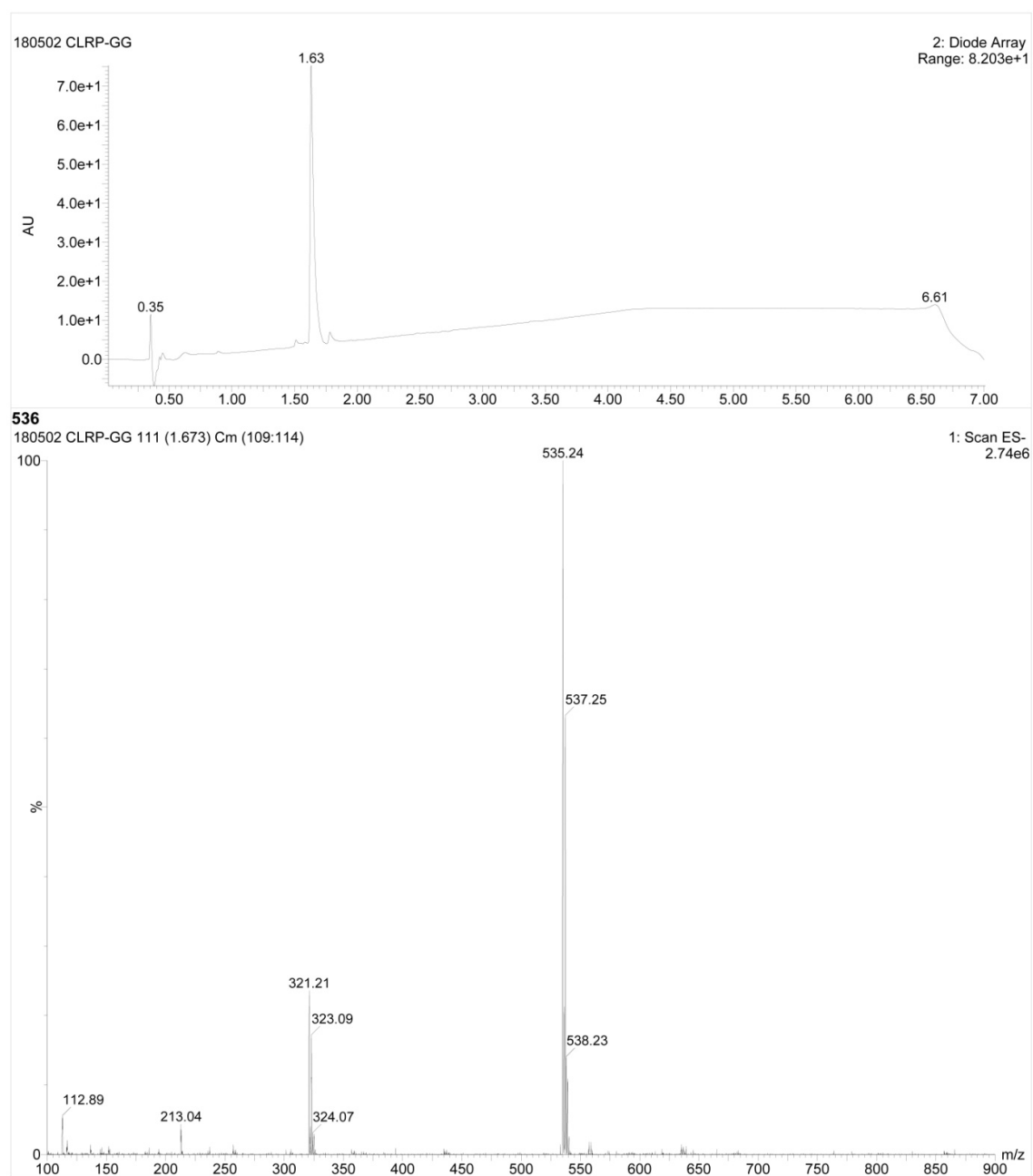


Figure S12. The LC (top) and Mass (bottom) spectrum of CLsuGG (**3**), $[M-H]^-$ at m/z 535.

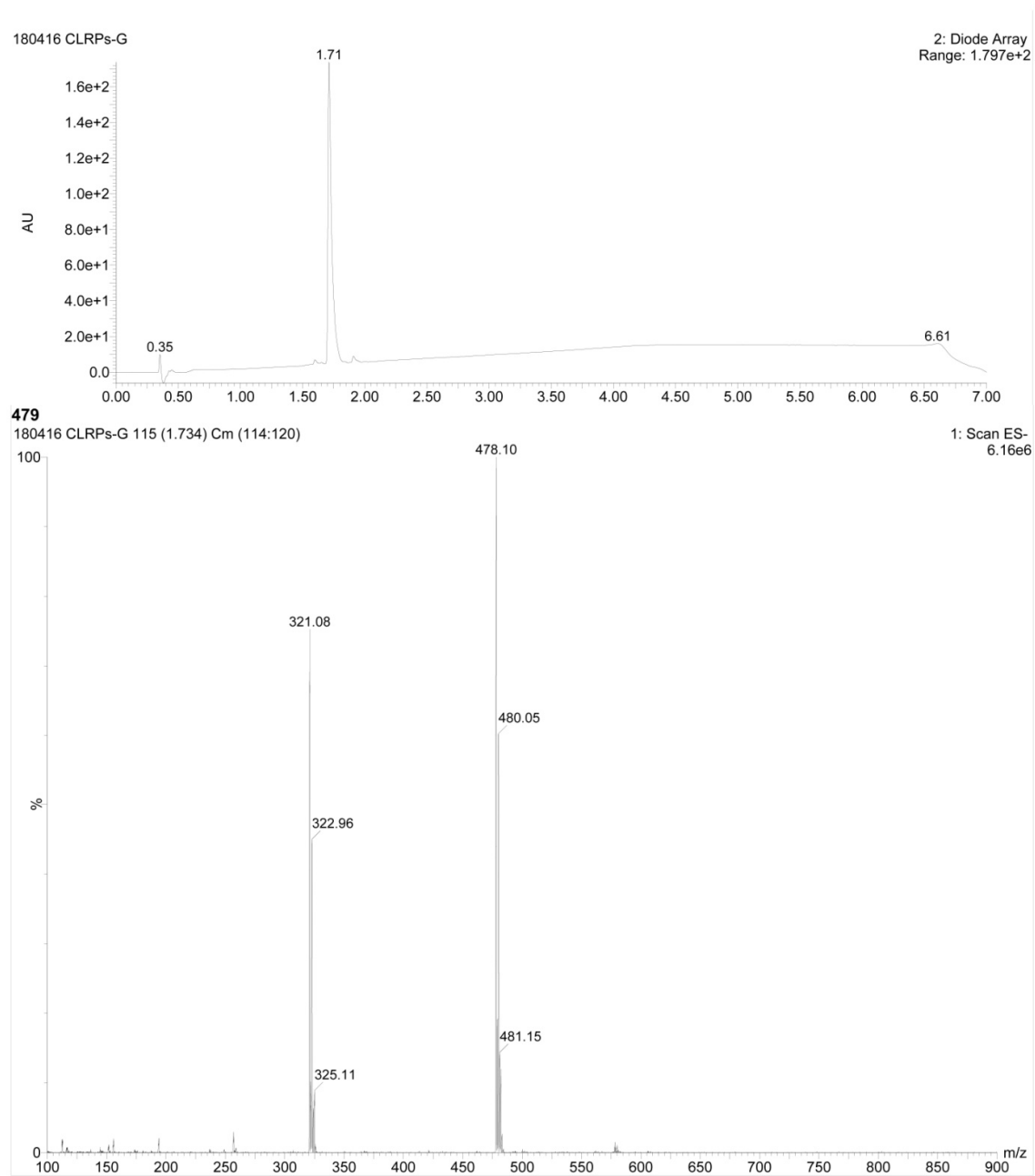


Figure S13. The LC (top) and Mass (bottom) spectrum of CLSuG (4), $[M-H]^-$ at m/z 478.

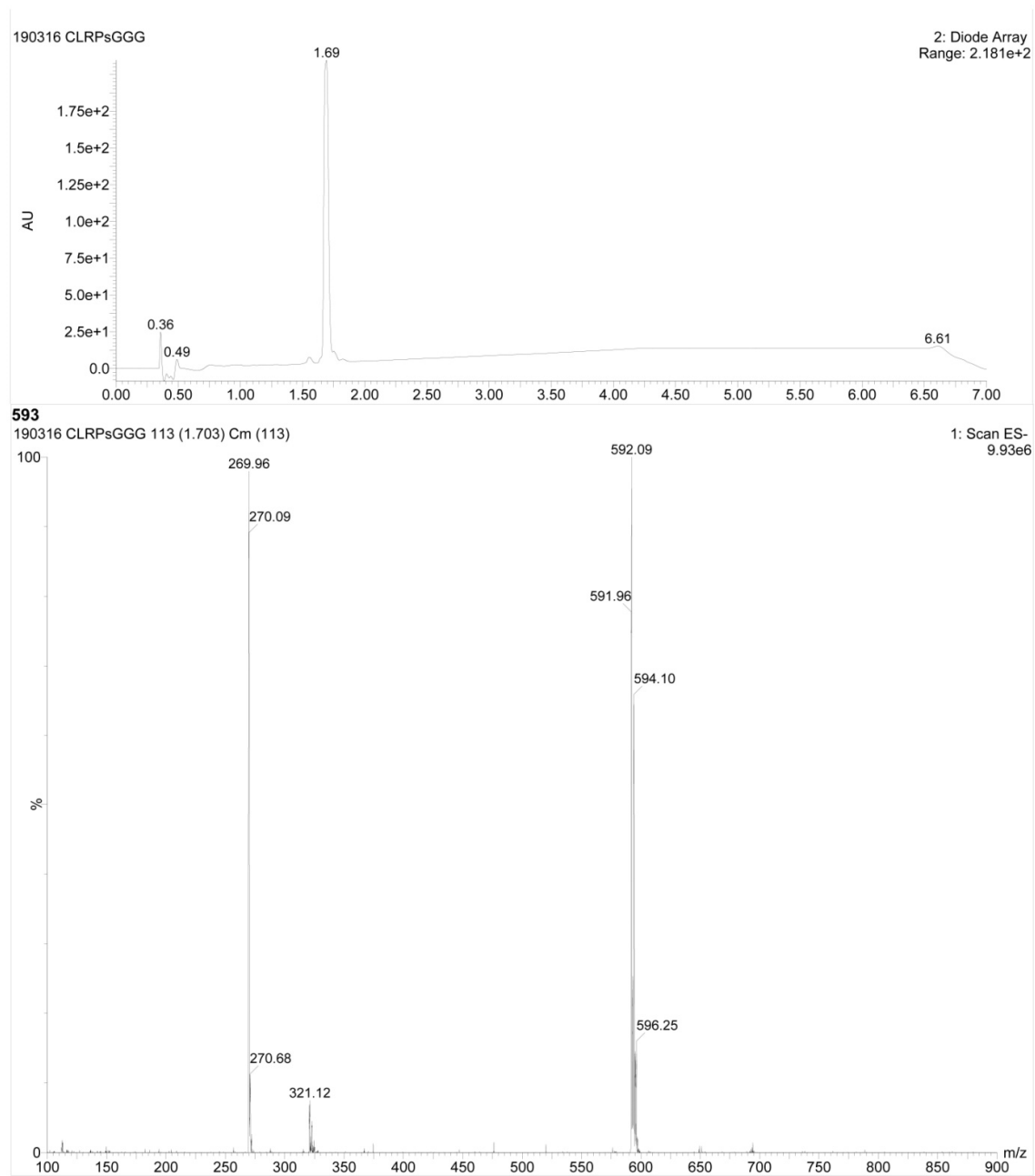


Figure S14. The LC (top) and Mass (bottom) spectrum of CLsuGGG (5), [M-H]⁻ at *m/z* 592.

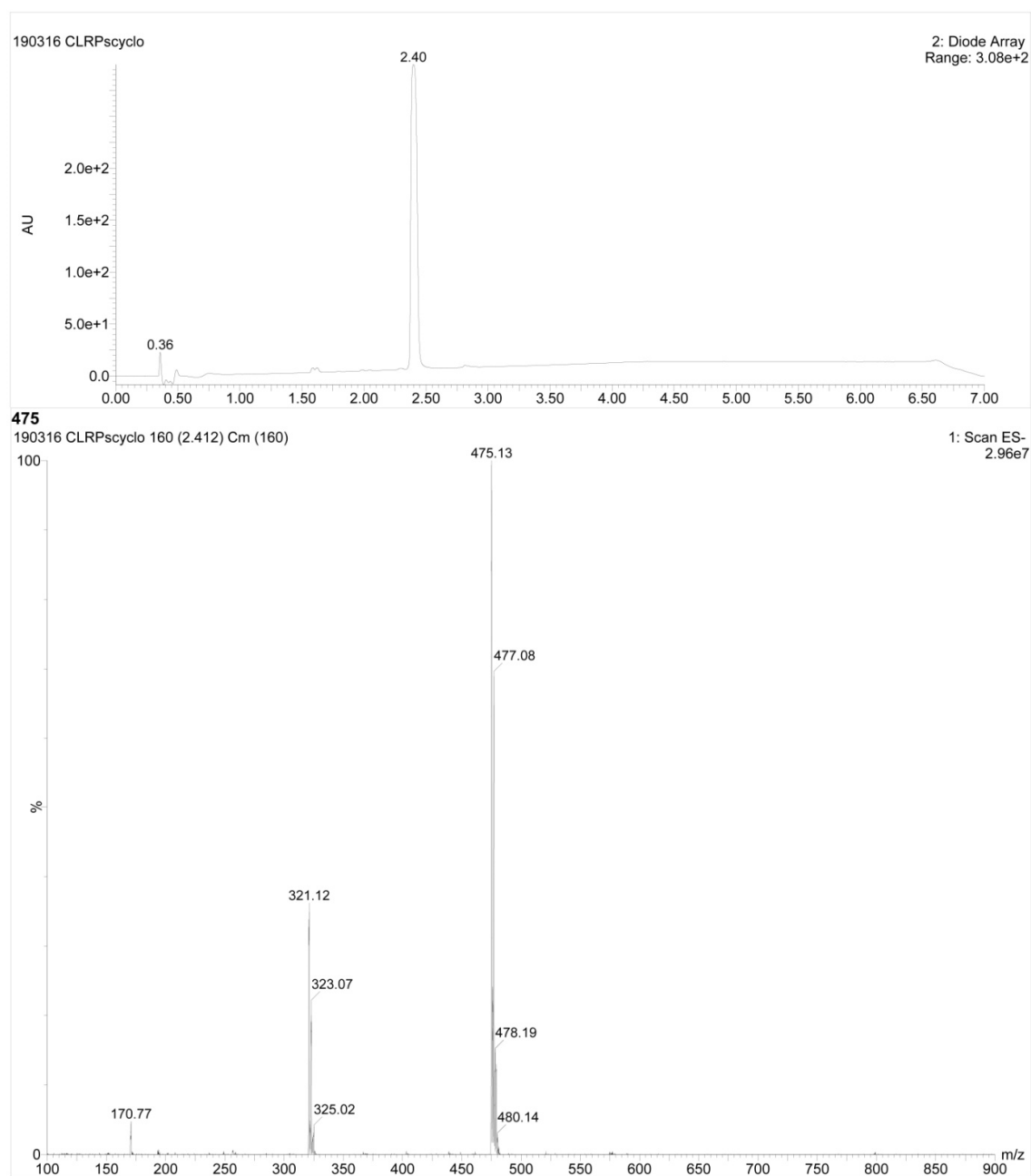


Figure S15. The LC (top) and Mass (bottom) spectrum of **6**, $[M-H]^-$ at m/z 475.

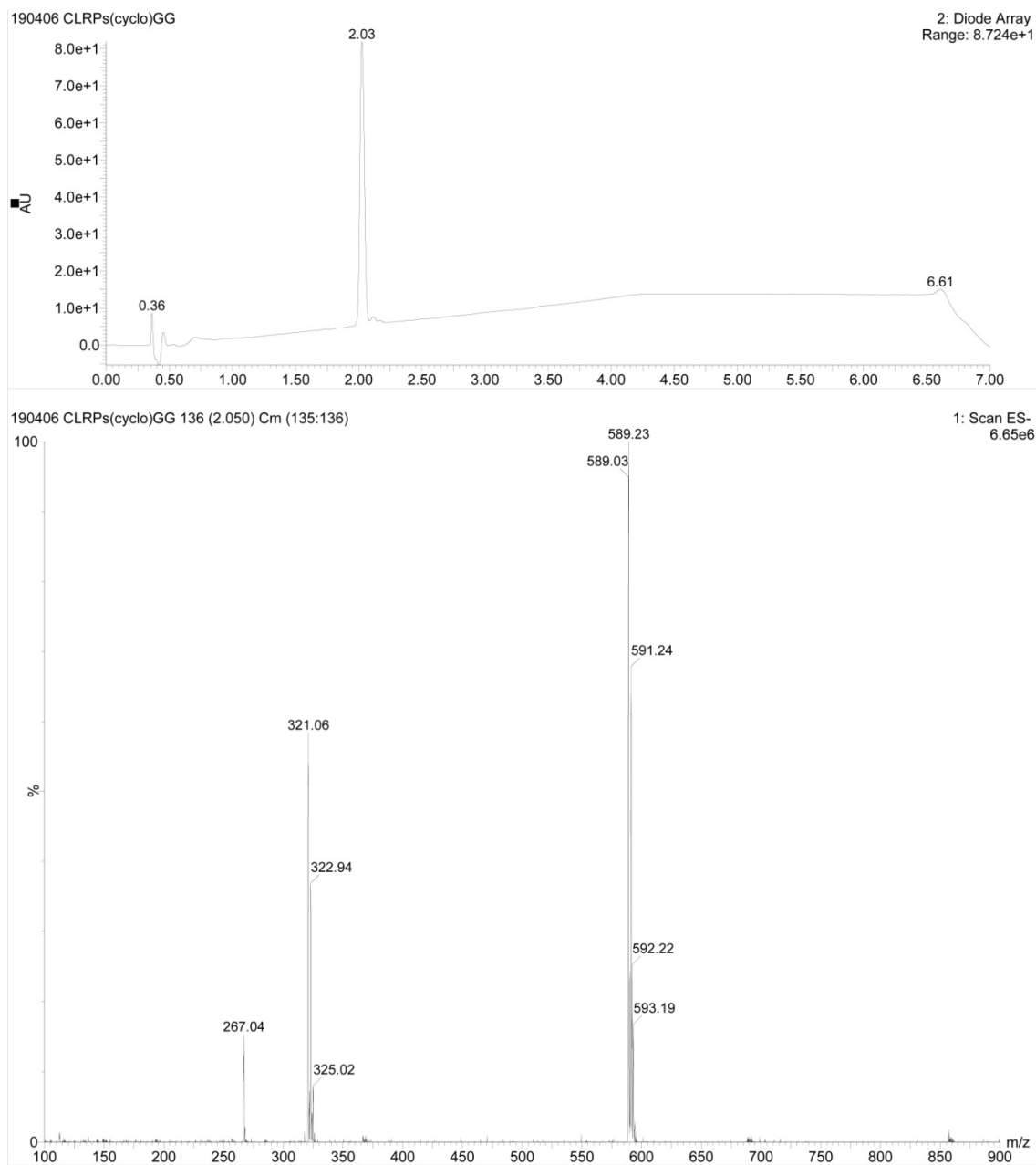


Figure S16. The LC (top) and Mass (bottom) spectrum of **7**, $[M-H]^-$ at m/z 589.

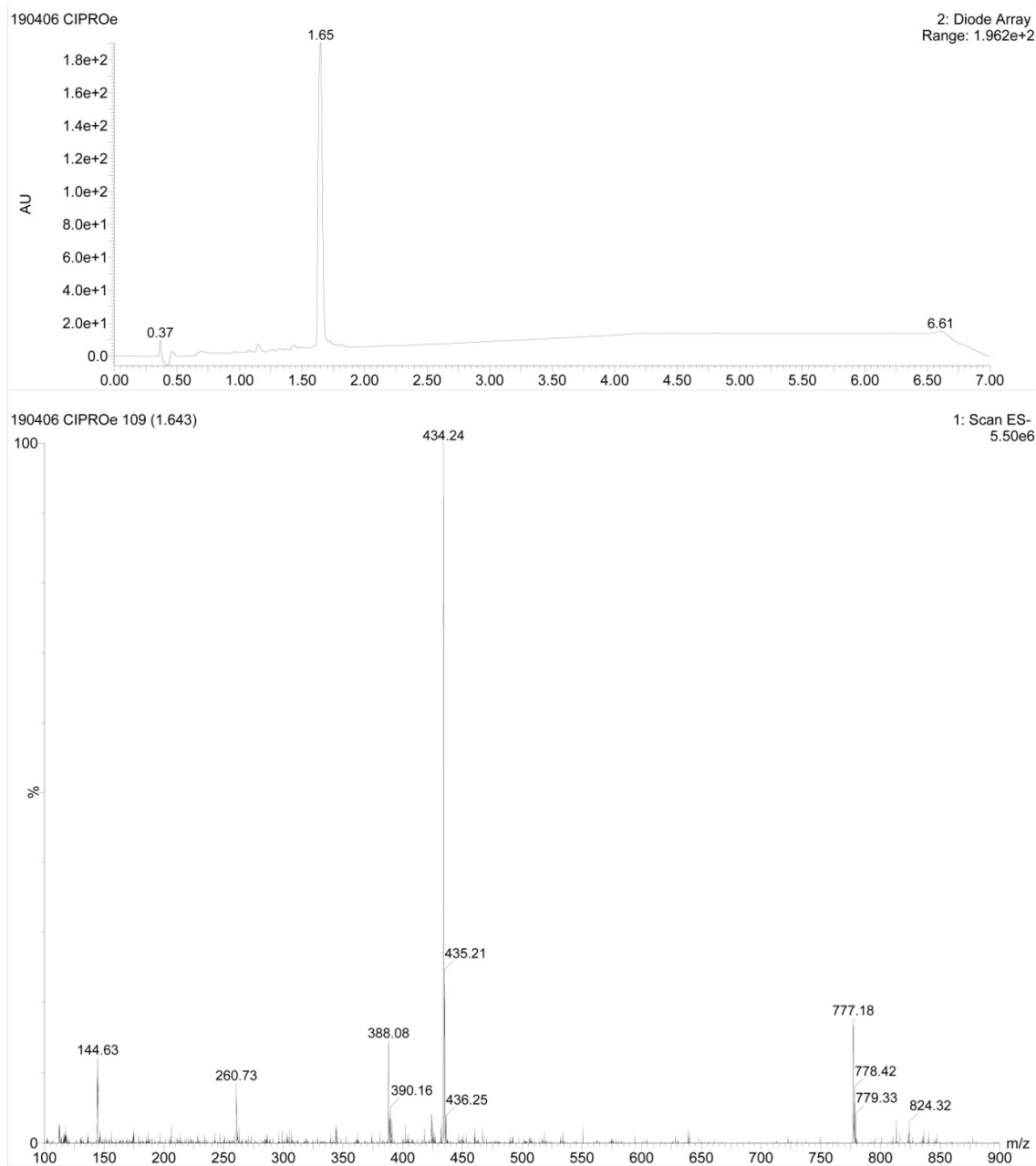


Figure S17. The LC (top) and Mass (bottom) spectrum of **8**, $[M-H]^-$ at m/z 388. The m/z 777 $[M-H]^-$ is the dimer of **8**.

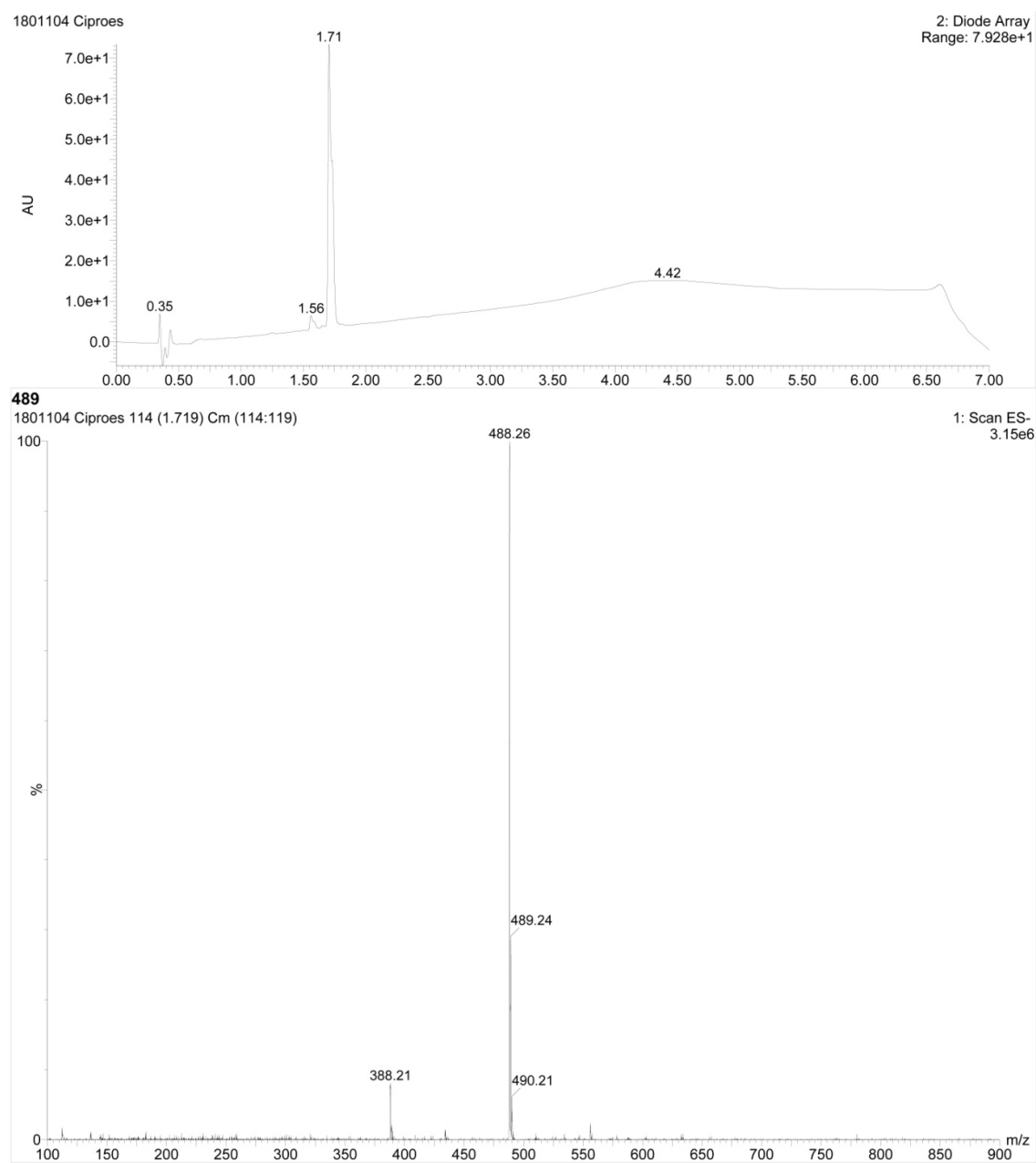


Figure S18. The LC (top) and Mass (bottom) spectrum of **9**, $[M-H]^-$ at m/z 488.

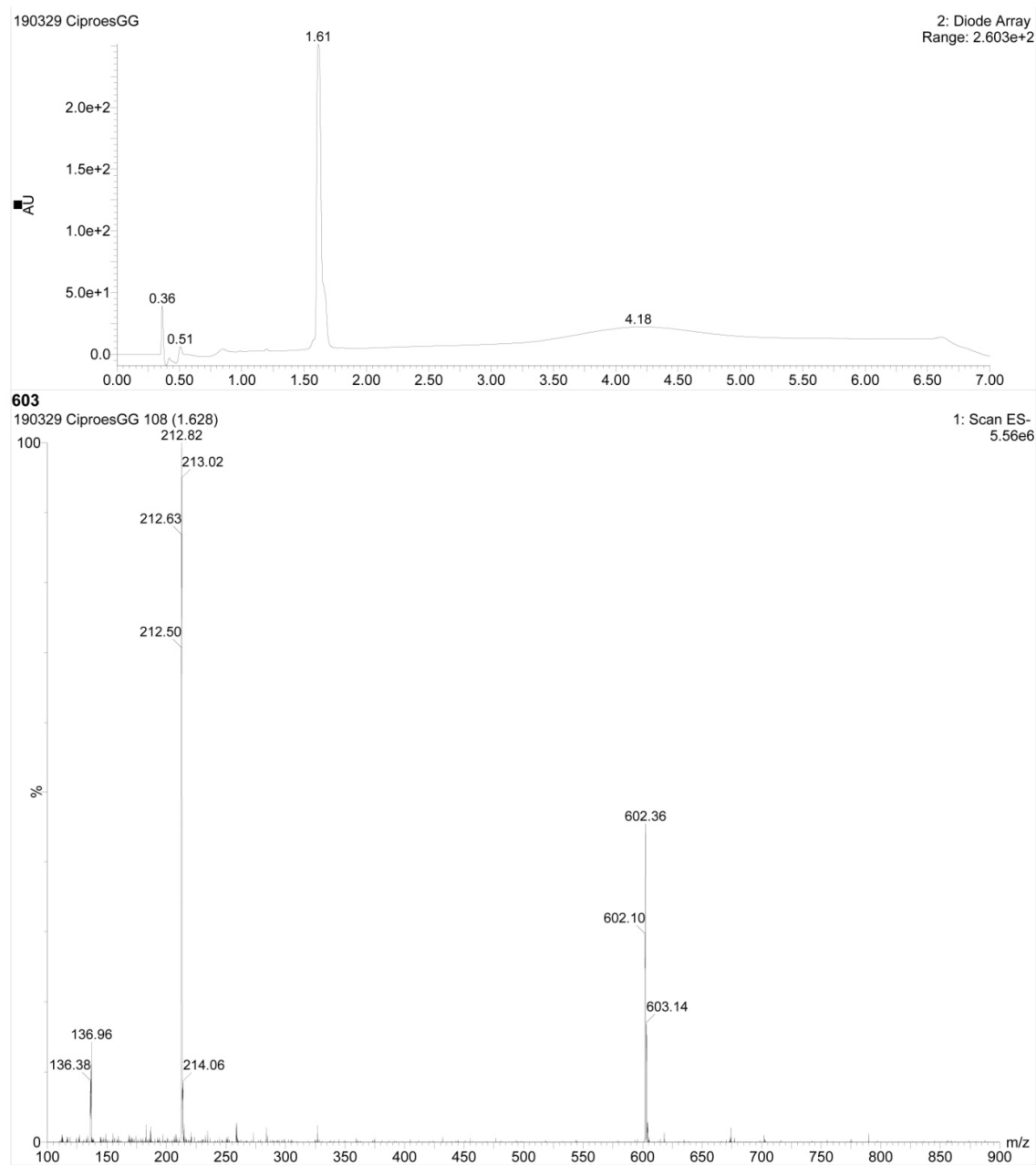


Figure S19. The LC (top) and Mass (bottom) spectrum of **10**, [M-H]⁻ at *m/z* 602.

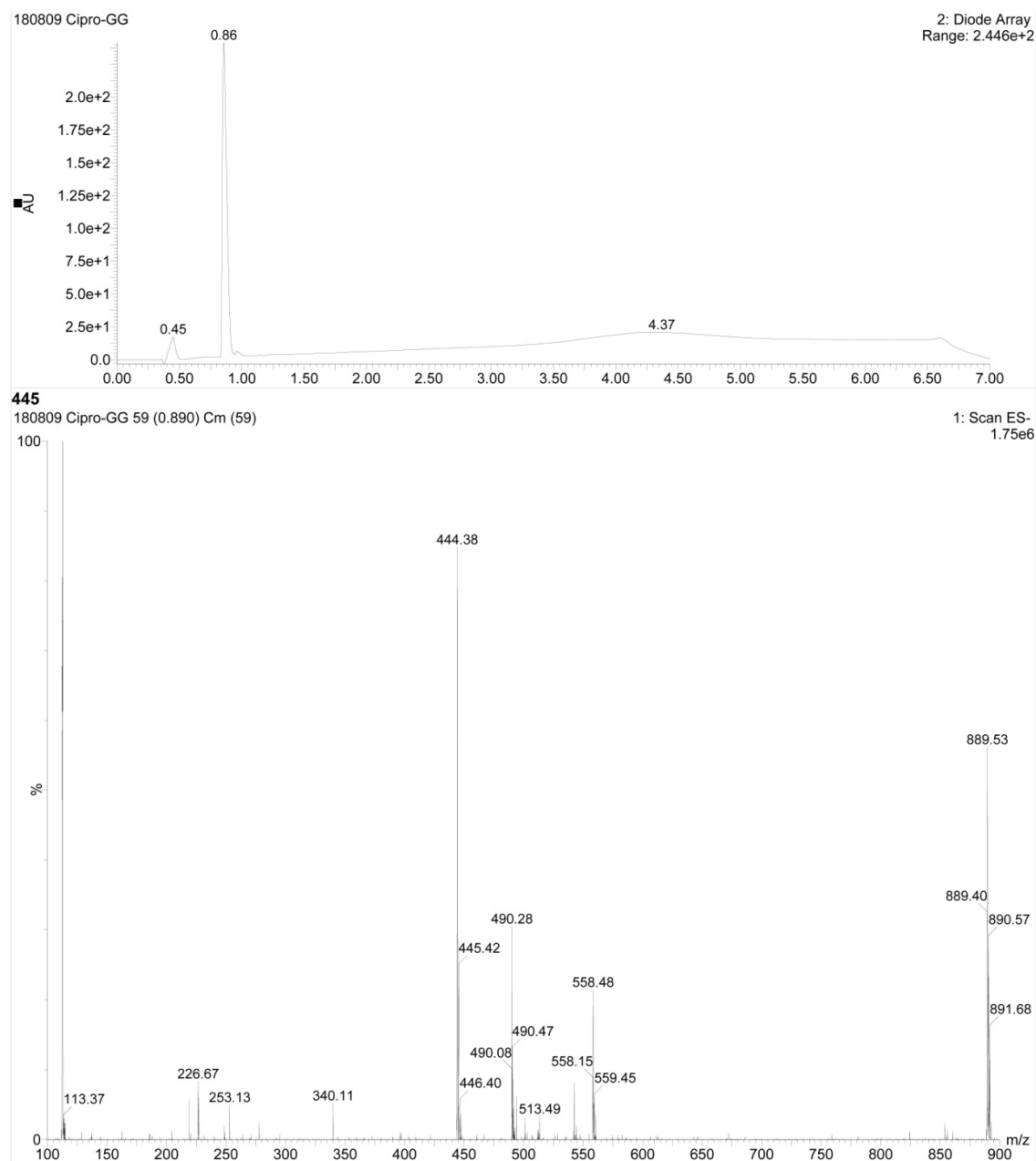


Figure S20. The LC (top) and Mass (bottom) spectrum of **11**, [M-H]⁻ at m/z 444. The m/z 889 [M-H]⁻ is the dimer of **11**.

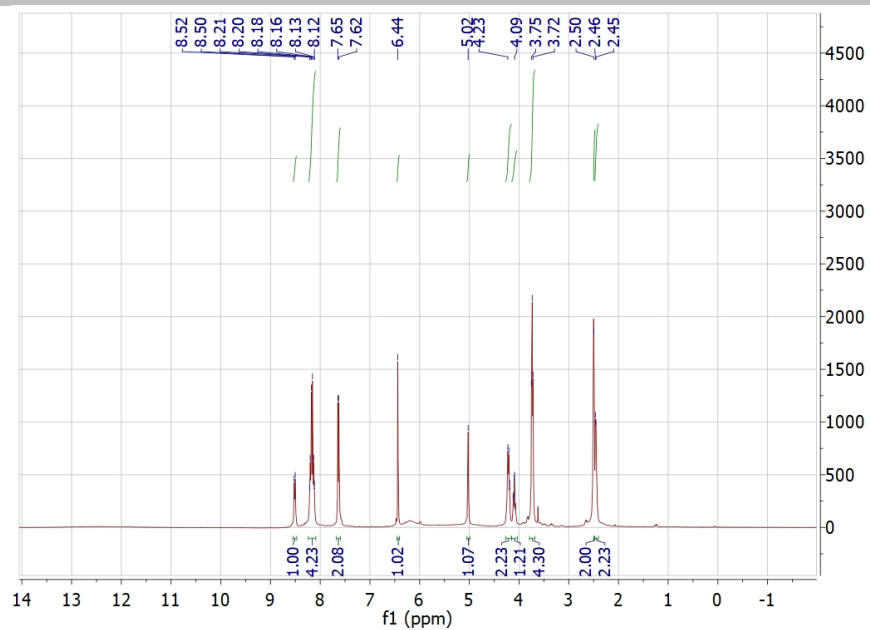


Figure S21. ¹H NMR of CLsuGG (3) in DMSO-*d*₆.

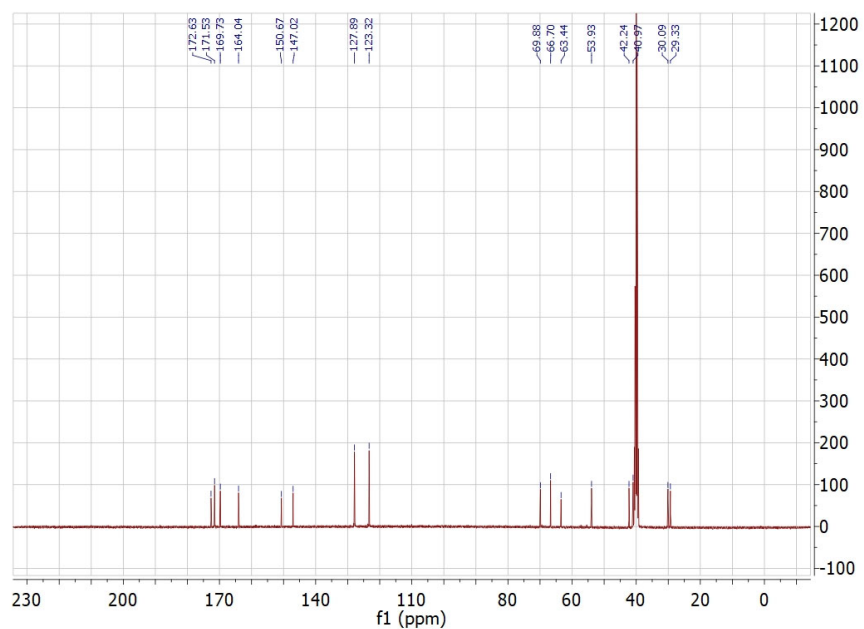


Figure S22. ¹³C NMR of CLsuGG (3) in DMSO-*d*₆.

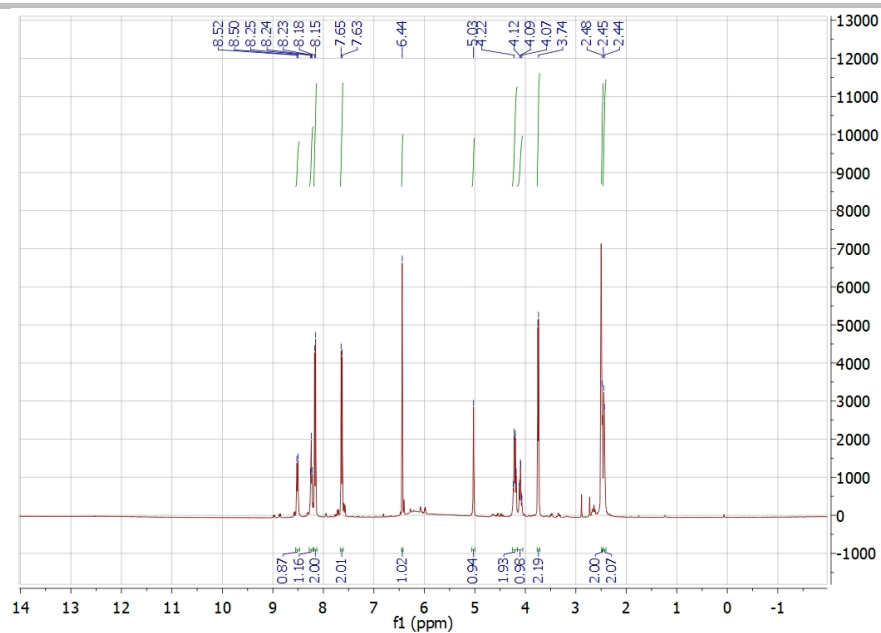


Figure S23. ¹H NMR of CLsuG (4) in DMSO-*d*₆.

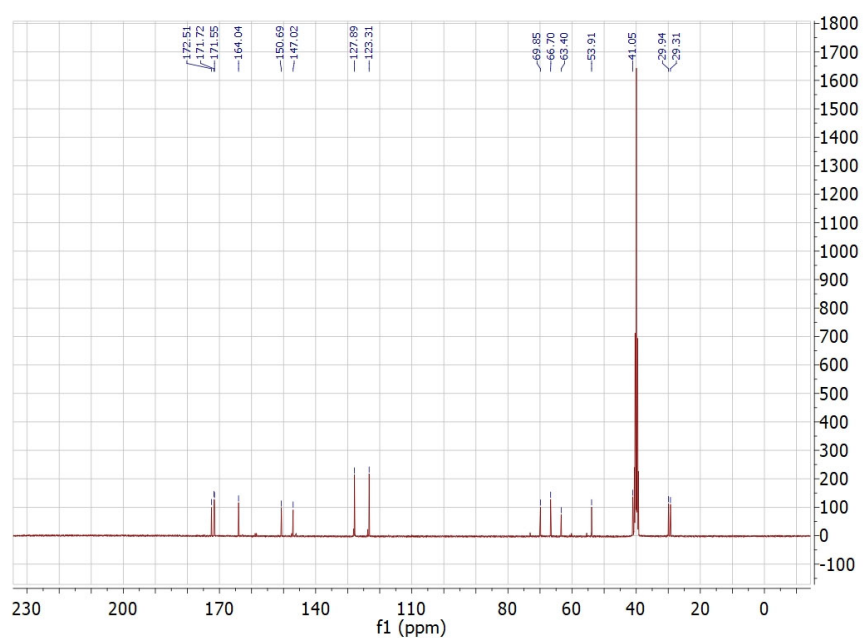


Figure S24. ¹³C NMR of CLsuG (4) in DMSO-*d*₆.

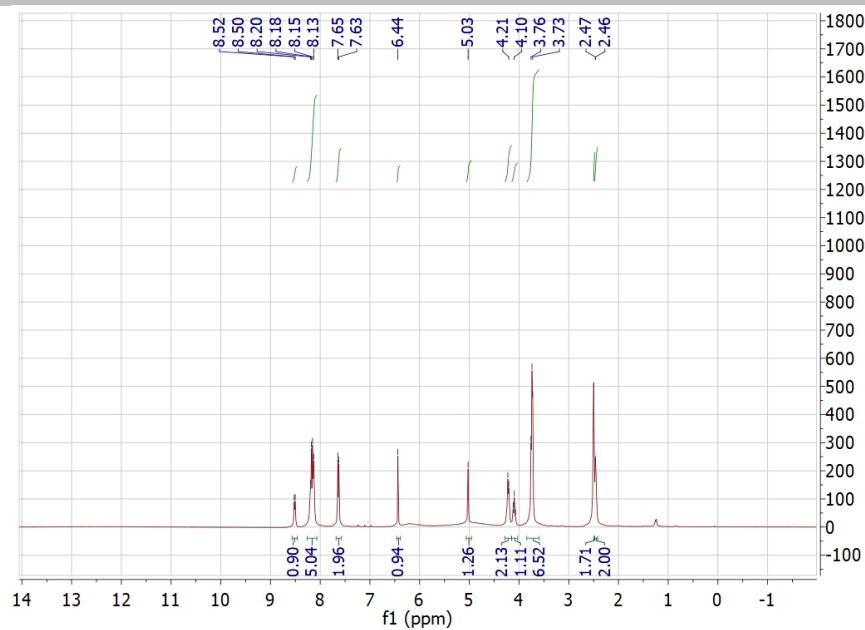


Figure S25. ¹H NMR of CLsuGGG (5) in DMSO-*d*₆.

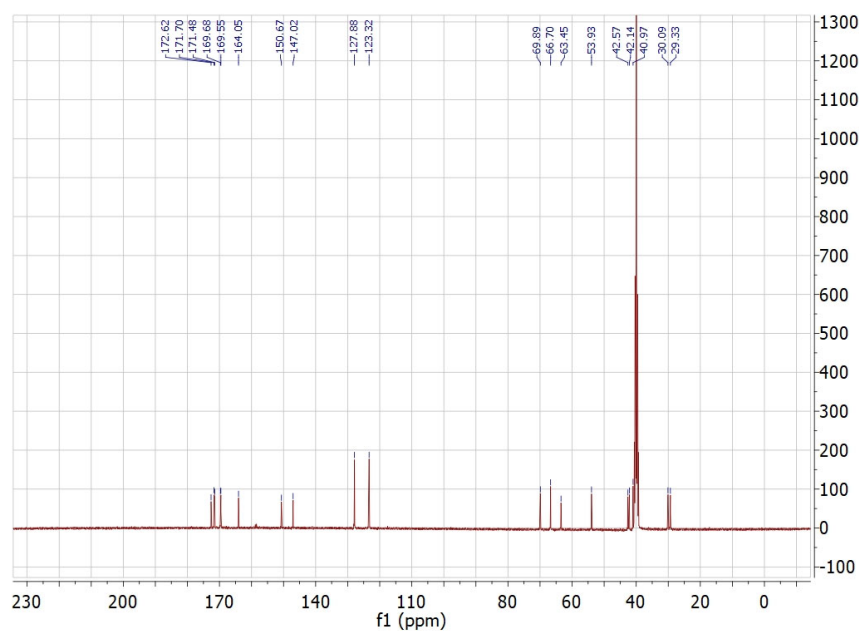


Figure S26. ¹³C NMR of CLsuGGG (5) in DMSO-*d*₆.

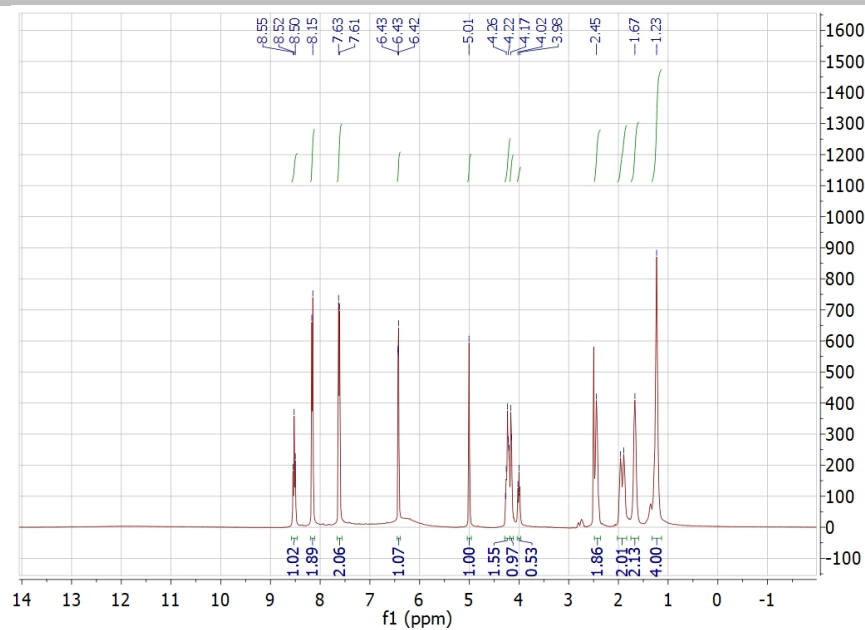


Figure S27. ¹H NMR of 6 in DMSO-*d*₆.

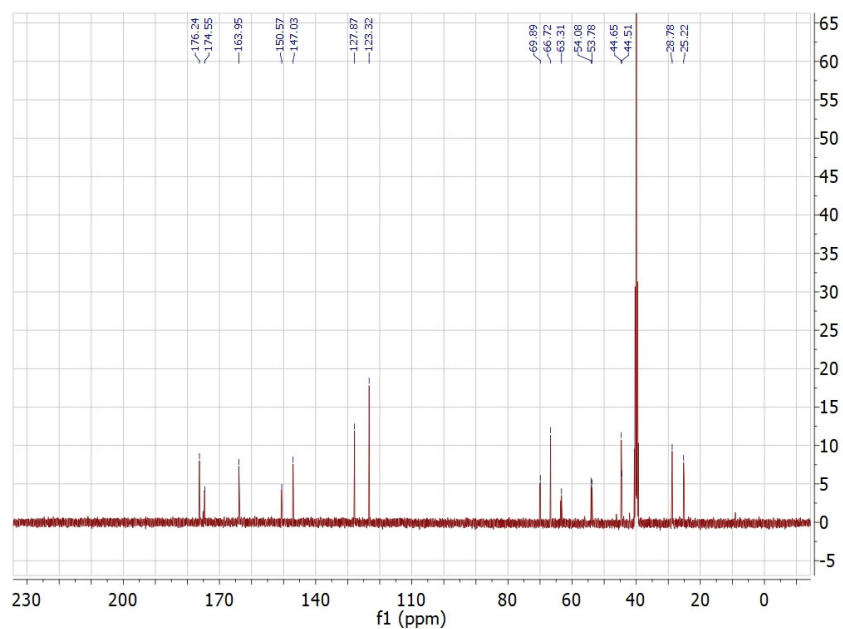


Figure S28. ¹³C NMR of 6 in DMSO-*d*₆.

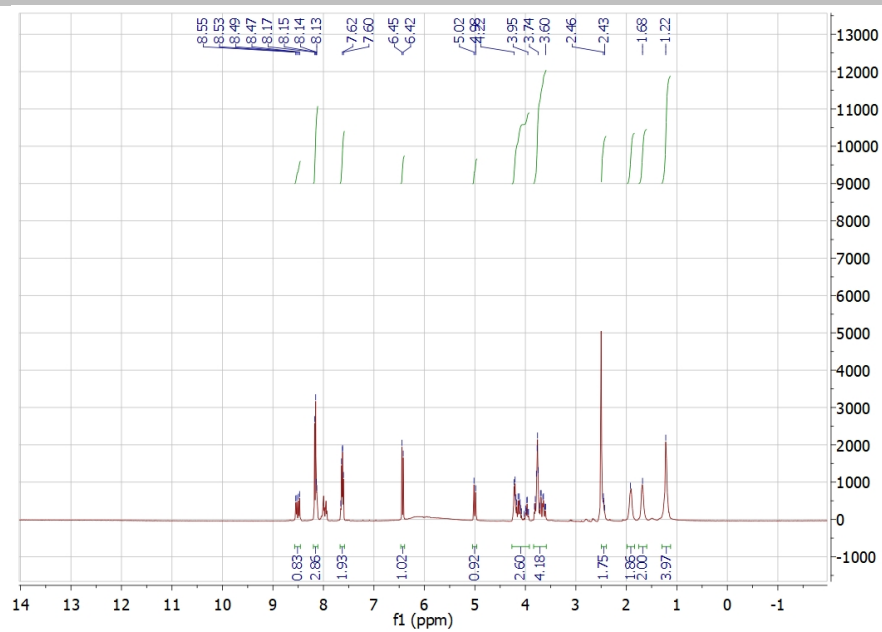


Figure S29. ¹H NMR of 7 in DMSO-*d*₆.

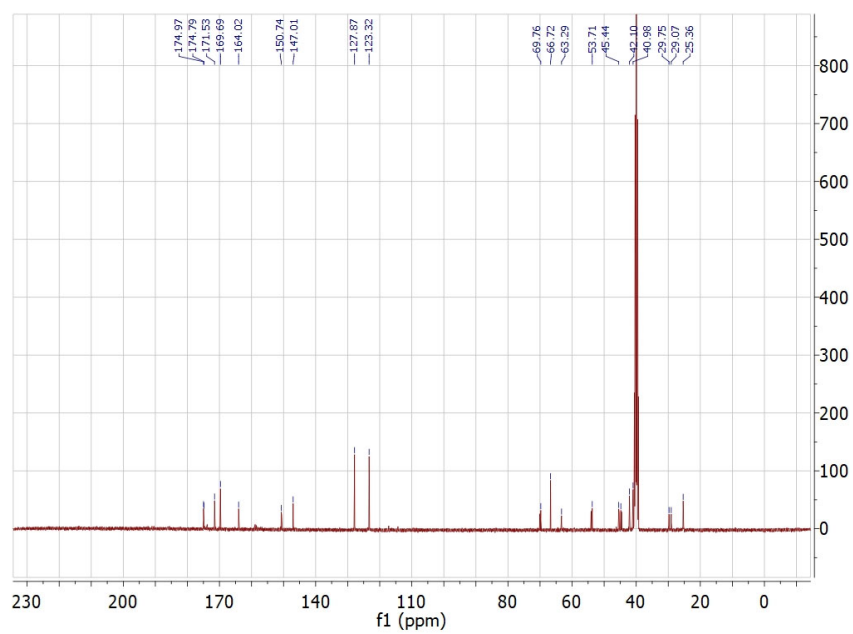


Figure S30. ¹³C NMR of 7 in DMSO-*d*₆.

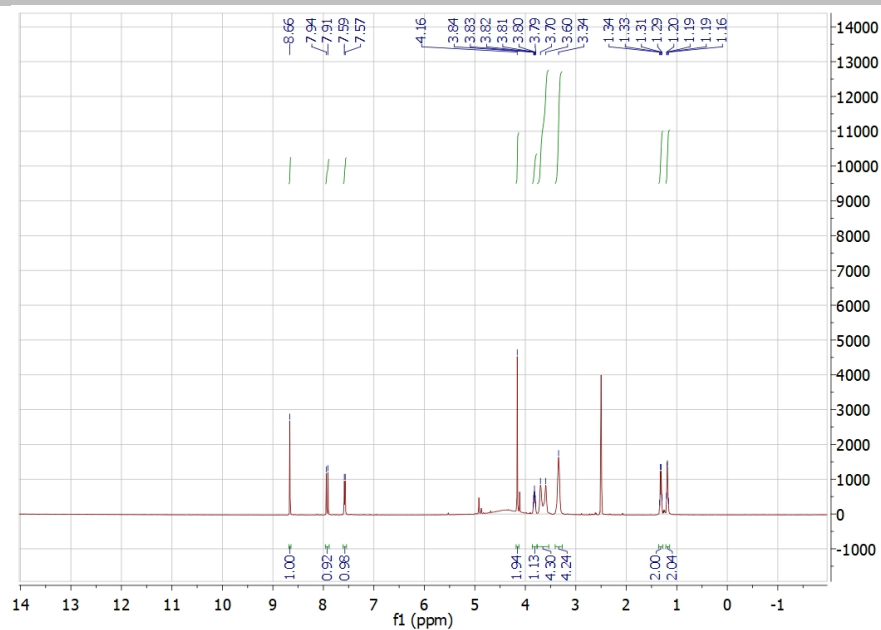


Figure S31. ¹H NMR of **8** in DMSO-*d*₆.

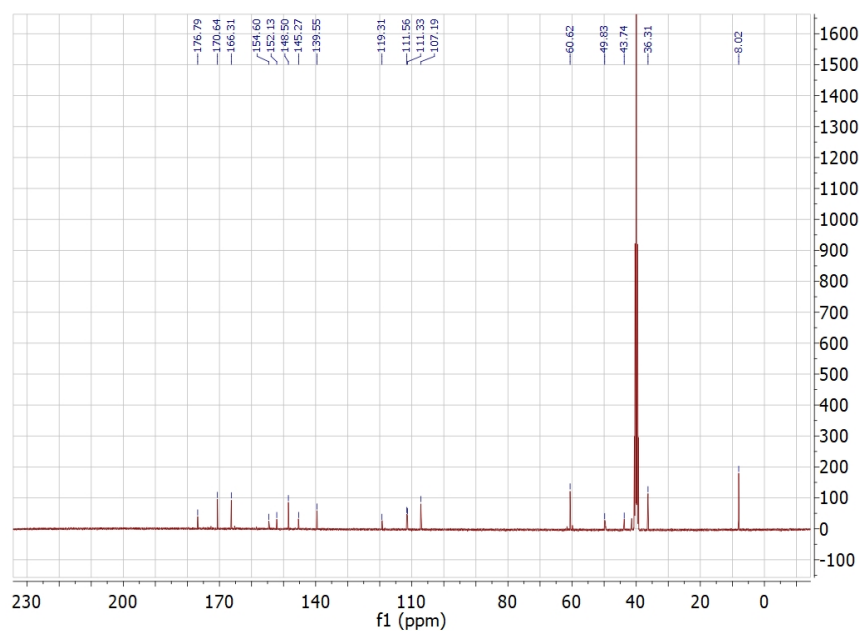


Figure S32. ¹³C NMR of **8** in DMSO-*d*₆.

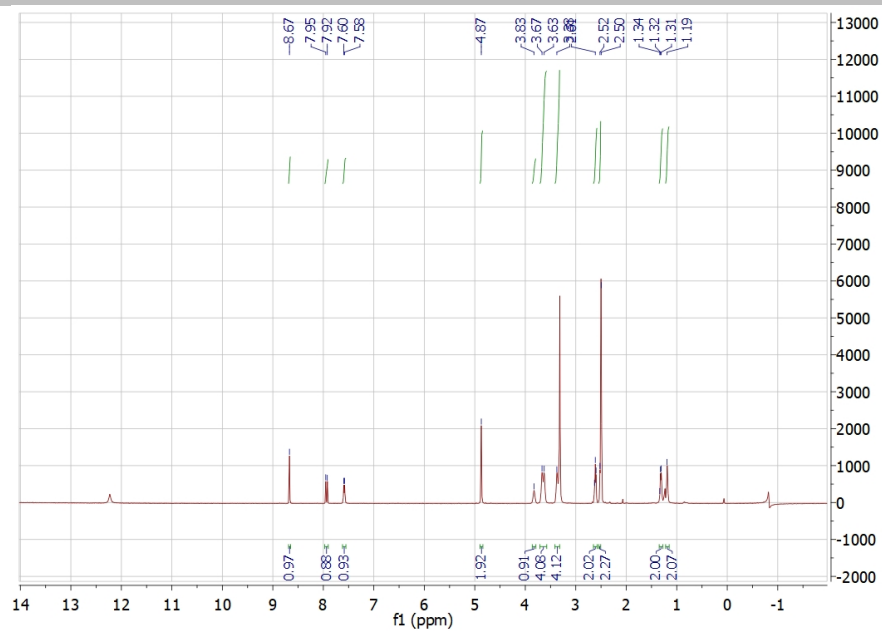


Figure S33. ¹H NMR of **9** in DMSO-*d*₆.

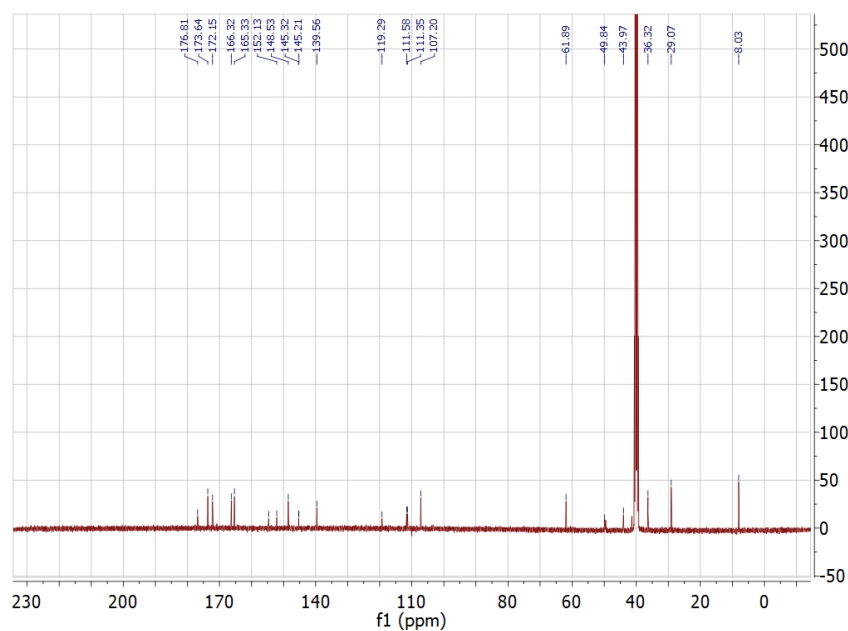


Figure S34. ¹³C NMR of **9** in DMSO-*d*₆.

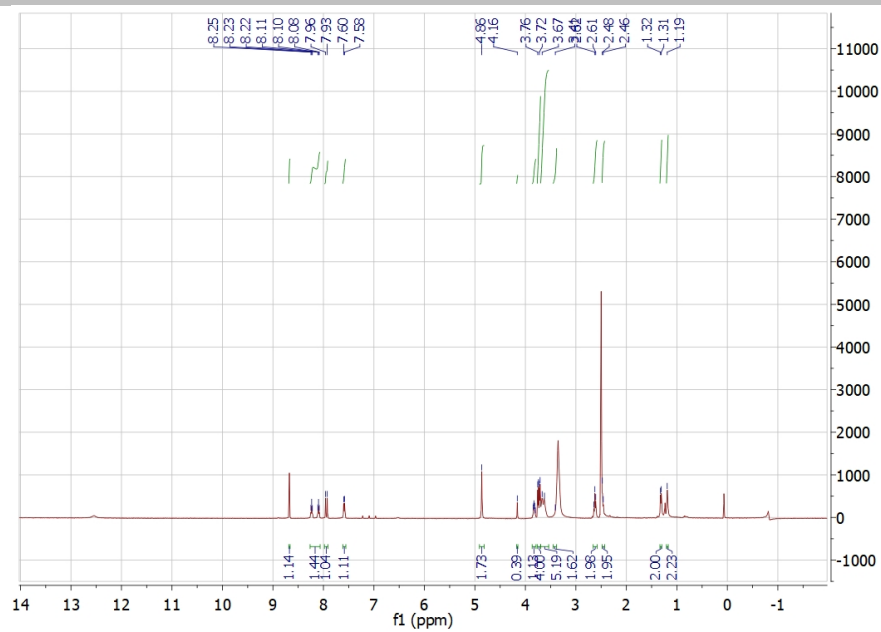


Figure S35. ¹H NMR of **10** in DMSO-*d*₆.

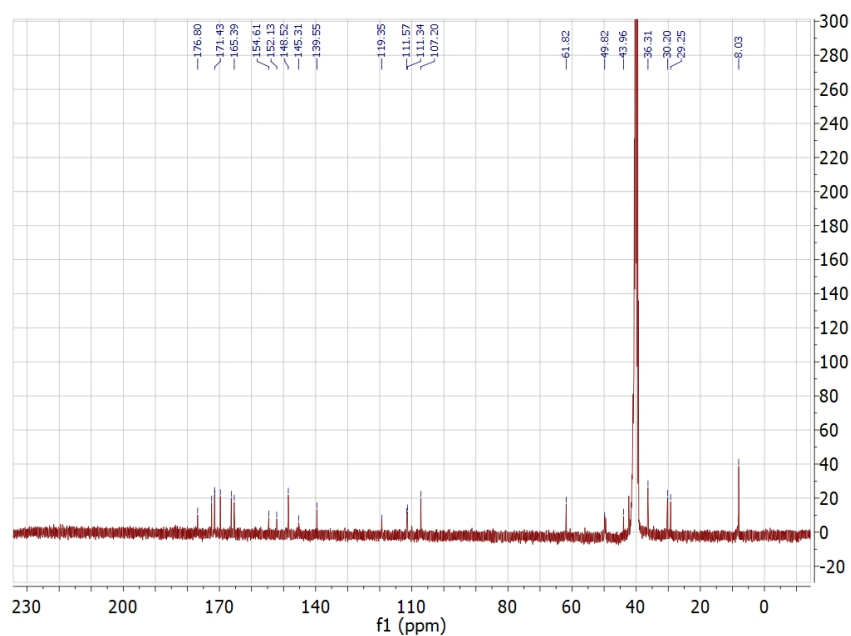


Figure S36. ¹³C NMR of **10** in DMSO-*d*₆.

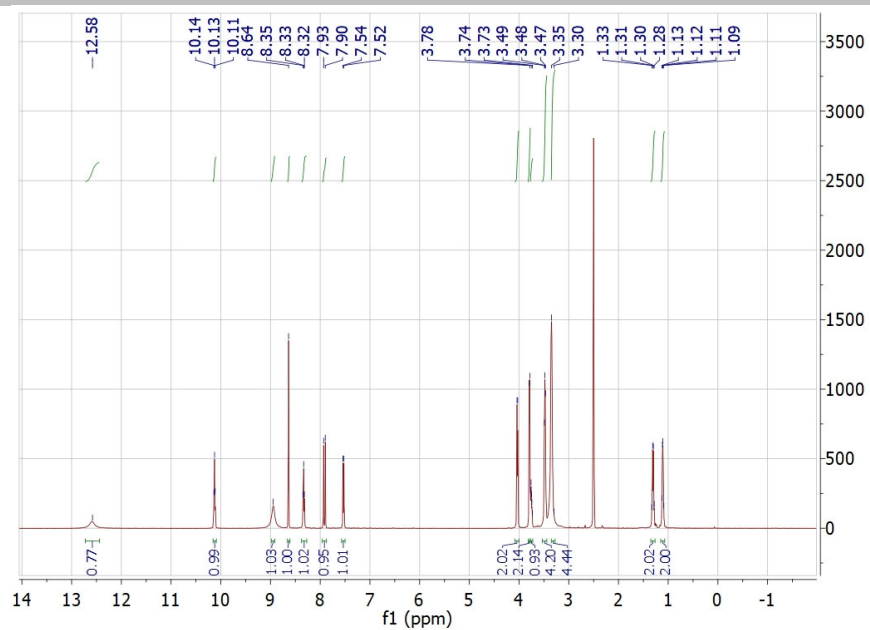


Figure S37. ^1H NMR of **11** in $\text{DMSO-}d_6$.

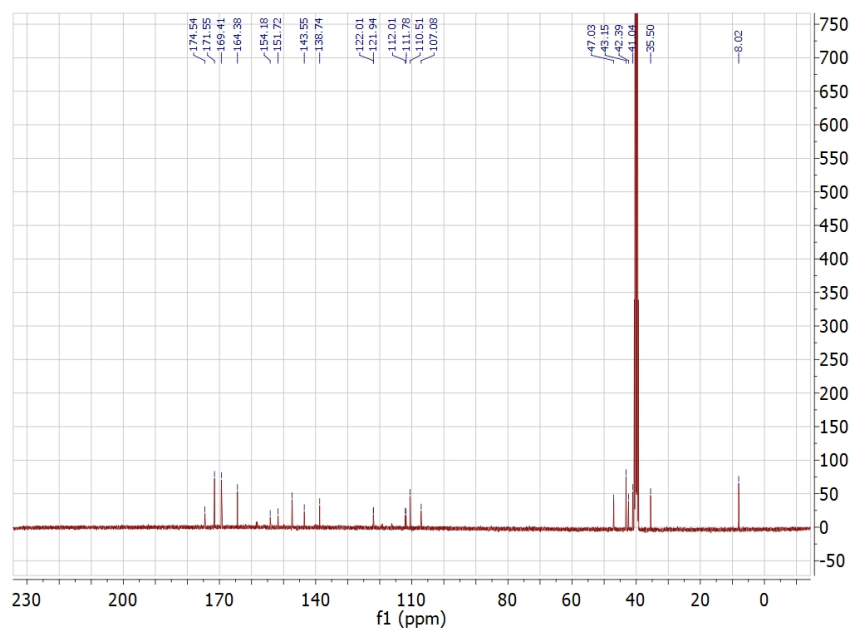


Figure S38. ^{13}C NMR of **11** in $\text{DMSO-}d_6$.

References

- [1] W. C. Chan, P. D. White, Oxford: Oxford University Press, **2000**.
- [2] R. De La Fuente, N. Sonawane, D. Arumainayagam, A. Verkman, *Br. J. Pharmacol*, **2006**, *149*, 551-559.